11 Models for Development and Pattern Formation in Biological Systems

It is suggested that a system of chemical substances, called morphogens, reacting together and diffusing through a tissue, is adequate to account for the main phenomena of morphogenesis.
A. M. Turing, (1952).
The chemical basis for morphogenesis.
Phil. Trans. Roy. Soc. Lond., 237, 37–72.

. . . Simple interactions can have consequences that are not predictable by intuition based on biological experience alone.
L. A. Segel, (1980). ed.
Mathematical Models in Molecular and Cellular Biology,
Cambridge University Press, Cambridge, England.

This indicates a genuine developmental constraint, namely that it is not possible to have a striped animal with a spotted tail . . .
J. D. Murray (1981a).

The beauty of natural forms and the intricate shapes, structures, and patterns in living things have been a source of wonder for natural philosophers long before our time. Like the spiral arrangement of leaves or florets on a plant, the shapes of shells, horns, and tusks were thought to signify some underlying geometric concepts in Na-

ture's designs. The teeming world of minute organisms was found to hold patterns no less amazing than those on the grander scales. Forms of living things were used from ancient times as a means of classifying relationships among organisms. The study of phenomena underlying such forms, although more recent, also dates back to previous centuries.

Initially, a primary fascination with static designs was characterized by attempts to fathom the secrets of natural forms with geometric concepts or simple physical analogies. *Phyllotaxis* (the study of the geometric arrangement of plant parts; e.g. leaves on a stem, scales on a cone, etc.) was then restricted to classification of spiral patterns on the basis of mathematical sequences (such as the Fibonacci numbers). The shapes of minute aquatic organisms and the structures created by successive cell divisions were compared to those formed by soap bubbles suspended on thin wire frames. (Forces holding these shapes together were described formally by F. Plateau and P. S. Laplace in the 1800s.) Spiral growth was explained in the early 1900s by D. W. Thompson as a continuous addition of self-similar increments.

In recent times the emphasis has shifted somewhat in our study of development, differentiation, and morphogenesis (*morpho* = shape or form; *genesis* = formation) of living things. We have come to recognize that the forms of organisms, as well as the patterns on their leaves, coats, or scales, arise by complex dynamic processes that span many levels of organization, from the subcellular through to the whole individual. While detailed understanding is incomplete, some broad concepts are now recognized as underlying principles.

First, at some level, forms of organisms are genetically determined. Second, the final shape, design, or structure is usually a result of multiple stages of development, each one involving a variety of influences, intermediates, and chemical or physical factors. Third, dramatic events during development are sometimes due to rather gradual changes that culminate in sudden transitions. (This can be likened to a stroll that takes one unexpectedly over a precipice.) Finally, environmental influences and interactions with other organisms, cells, or chemicals can play nontrivial roles in a course of development.

There are numerous unrelated theories and models for differentiation and morphogenesis, just as there are many aspects to the phenomena. Here it would be impossible to give all these theories their due consideration, although some brief indications of references for further study are suggested in a concluding section. Instead of dealing in generalities, the discussion will be based on two rather interesting models for development and morphogenesis that are of recent invention.

In the first model we focus on the phenomenon of aggregation, a specific aspect of one unusually curious developmental system, the *cellular slime molds*. A partial differential equation (PDE) model due to Keller and Segel is described and analyzed. An explanation of several observations then follows from the mathematical results.

A second topic is then presented, that of chemical *morphogens*, (the putative molecular prepatterns that form signals for subsequent cellular differentiation). The theory (due to A. M. Turing) is less than 40 years old but stands as one of the single most important contributions mathematics has made to the realm of developmental biology.

While these topics are somewhat more advanced than those in the earlier chapters of this book, a number of factors combine to motivate their inclusion. From the pedagogic point of view, these are good illustrations of some analysis of PDE models. (While the analysis falls short of actually solving the equations in full generality, it nevertheless reveals interesting results.) Furthermore, techniques of linear stability methods, and the important concepts of gradual parameter variations (which are familiar to the reader) are reapplied here. (Although certain subtleties may require some guidance, the underlying philosophy and basic steps are the same.) This then is a final "variation on a theme" that threads it way through the approach to the three distinctly different types of models (discrete, continuous, and spatially distributed).

Even more to the point, the models presented here are examples of genuine insight that mathematics can contribute to biology. These case studies point to fundamental issues that would be difficult, if not impossible, to resolve based on verbal arguments and biological intuition alone. These examples reinforce the belief that theory may have an important role to play in the biological sciences.

The chapter is organized as follows: Sections 11.1 to 11.3 are devoted to the problem of aggregation. In particular, Section 11.2 introduces the methods of analyzing (spatially nonuniform) deviations from a (uniform) steady state. Readers who have not covered Chapters 9 and 10 in full detail can nevertheless follow this analysis provided that the equations of the model are motivated and that the form of the perturbations given by equations (9a,b) is taken at face value.

Sections 11.4 and 11.5 then introduce reaction-diffusion systems and chemical morphogens. The general model requires a very cursory familiarity with the diffusion equation (or faith that the special choice of perturbations given by equation (27) are appropriate; see motivation in Section 11.2). Further analysis is essentially straightforward given familiarity with Taylor series, eigenvalues, and characteristic equations. (A somewhat novel feature encountered is that the growth rate σ of perturbations depends on their spatial "waviness" q.) It is possible to omit the details of the derivation leading up to the conditions for diffusive instability, (32a,b) and (38), in the interest of saving time or making the material more accessible. Section 11.6 is an important one in which we use simple logical deductions to make physically interesting statements based on the conditions derived in the preceding analysis. The concepts in Section 11.7 are more subtle but lead to an appreciation of the role of the domain size on the chemical patterns. Implications for morphogenesis and for other systems are then given in Sections 11.8 and 11.9.

11.1 CELLULAR SLIME MOLDS

Despite their mildly repelling name, slime molds are particularly fascinating creatures offering an extreme example of "split personality." In its native state a slime mold population might consist of hundreds or thousands of unicellular amoeboid cells. Each one moves independently and feeds on bacteria by *phagocytosis* (i.e. by engulfing its prey). There are many species of slime molds commonly encountered in the soil; one of the most frequently studied is *Dictyostelium discoideum*.

When food becomes scarce, the amoebae enter a phase of starvation and an interesting sequence of events ensues. First, an initially uniform cell distribution develops what appear to be centers of organization called *aggregation sites*. Cells are attracted to these loci and move towards them, often in a pulsating, wavelike manner. Contacts begin to form between neighbors, and streams of cells converge on a single site, eventually forming a shapeless multicellular mass. The aggregate undergoes curious contortions in which its shape changes several times. For a while it takes on the appearance of a miniature slug that moves about in a characteristic way. The cells making up the forward portion become somewhat different biochemically from their colleagues in the rear. Already a process of differentiation has occurred; if left undisturbed the two cell types (called *prespore* and *prestalk*) will have quite distinct fates: Anterior cells turn into stalk cells while posterior cells become spores.

At this stage the differentiation of the multicellular mass is as yet reversible. A fascinating series of experiments (see box in Section 11.3) has been carried out to demonstrate that the ratio of the two cell types is self-regulating; if a portion of the slug is excised, some of the cells change their apparent type so as to preserve the proper ratio.

The sluglike collection of cells executes a crawling motion; understanding of the underlying mechanism is just beginning to emerge (see Odell and Bonner, 1986). It then undertakes a sequence of shapes including that of a dome. As a culmination of this amazing sequence of events, cellular streaming resembling a "reverse fountain" brings all prestalk cells around the outside and down through the center of the mass. The result is a slender, beautifully sculptured stalk bearing a spore-filled capsule at its top. In order to provide a rigid structural basis, the stalk cells harden and eventually die. The spore cells are thereby provided with an opportunity to survive the harsh conditions, to be dispersed by air currents, and to thus propagate the species into more favorable environments. Since individual slime mold cells do not reproduce after the onset of aggregation, there is always some fraction of the population that is destined to die as part of the structural material. (There is a natural tendency to view this anthropomorphically as an example of self-sacrifice for the group interest.)

Slime molds have fascinated biologists for many decades, not simply for their amazing repertoire, but also because of their easily accessible and malleable developmental system. There are many intriguing questions to be addressed in understanding the complicated social behavior of this population of relatively primitive organisms. To outline just a few theoretical questions, consider:

1. What causes cells to aggregate, and how do cells "know" where an aggregation center should form?
2. What mechanisms underly motion in the slug?
3. What determines the prespore-prestalk commitment, and how is the ratio controlled? (This is a problem of size regulation in a pattern.)
4. How are cells sorted so that prestalk and prespore cells fall into appropriate places in the structure?
5. What forces lead to the formation of a variety of shapes including that of the final *sporangiophore* (the spore-bearing structure)?

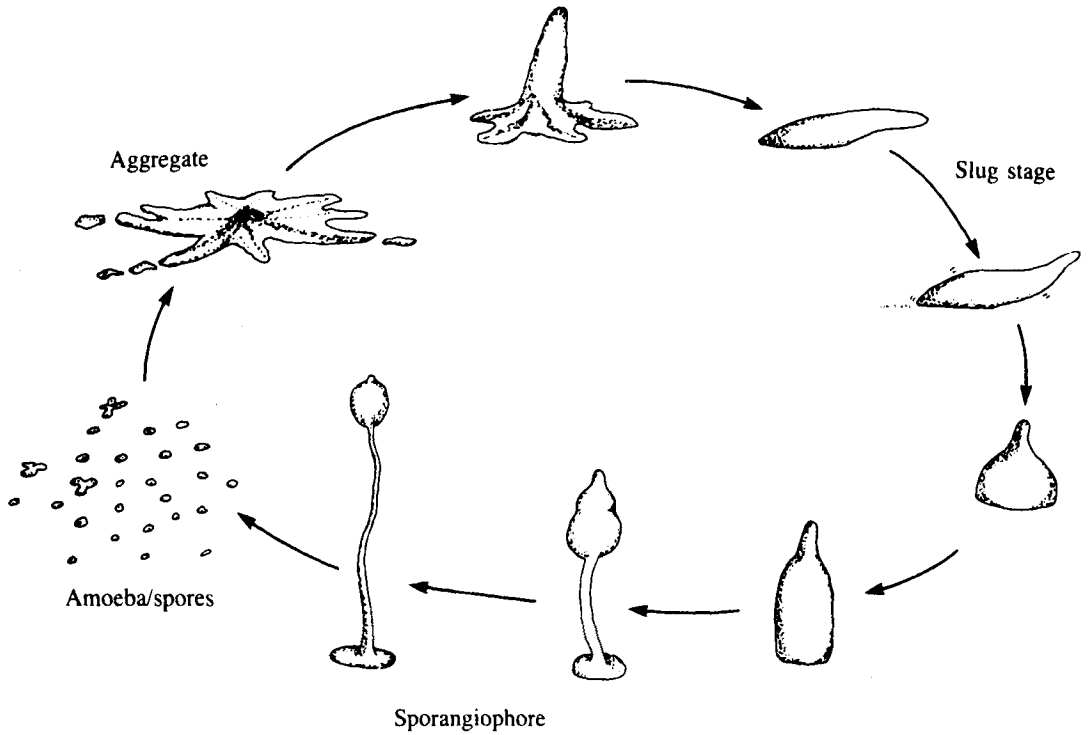

Figure 11.1 *Life cycle of the slime mold* Dictyostelium discoideum *showing the sequence of events leading to formation of the spore-bearing stalk, the sporangiophore.*

While the theoretical literature deals with such questions, we shall address only the first of these. (Other topics are excellent material for advanced independent study.) Perhaps best understood to date, the aggregation process has been rather successfully analyzed by Keller and Segel (1970) in a mathematical model that leads to a more fundamental appreciation of this key step in the longer chain of events.

For many years it has been known that starved slime mold amoebae secrete a chemical that attracts other cells. Initially named acrasin, it was subsequently identified as *cyclic AMP* (cAMP), a ubiquitous molecule whose role is that of an intracellular messenger. The cells also secrete *phosphodiesterase,* an enzyme that degrades cAMP. cAMP secretion is autocatalytic in the sense that free extracellular cAMP promotes further cAMP secretion by a chain of enzymatic reactions (in which a membrane-bound enzyme, *adenylate cyclase,* is implicated). The molecular system has been studied in some depth (see references).

To give a minimal model for the aggregation phase, Keller and Segel (1970) made a number of simplifying assumptions:

1. Individual cells undergo a combination of random motion and chemotaxis towards cAMP.
2. Cells neither die nor divide during aggregation.
3. The attractant cAMP is produced at a constant rate by each cell.

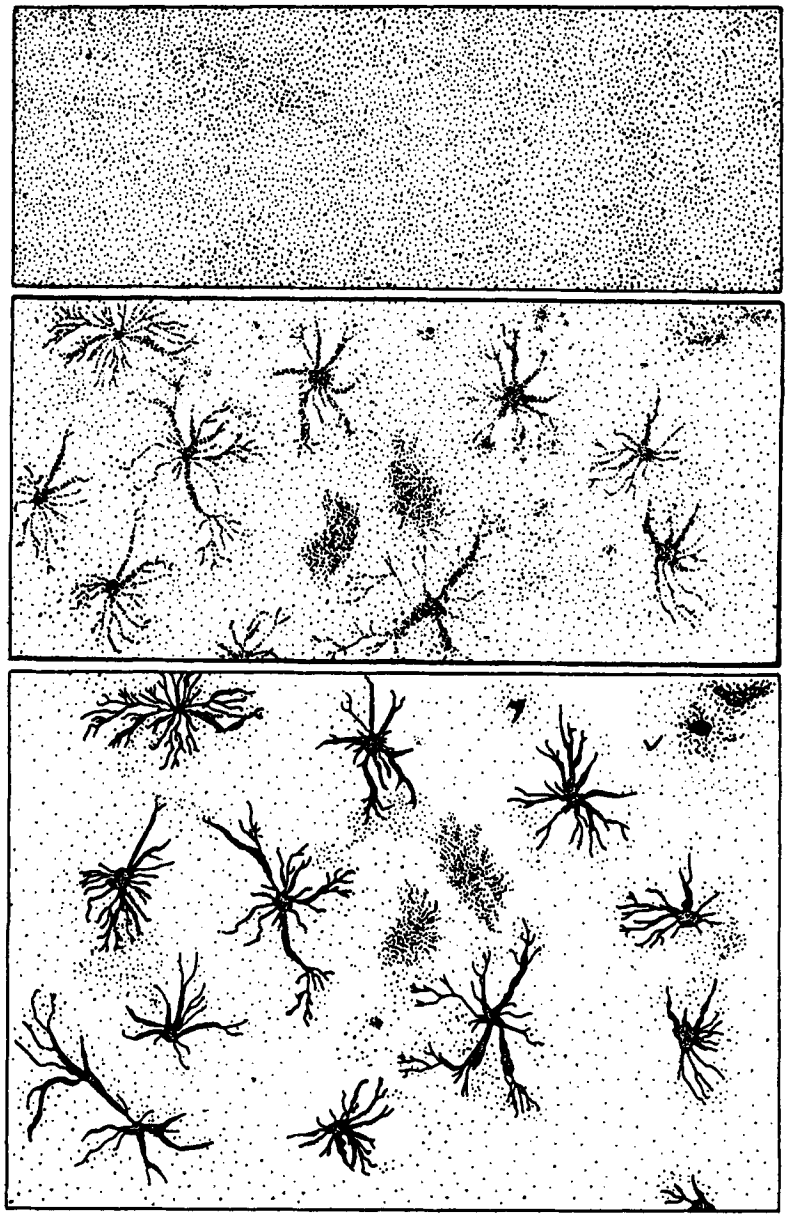

Figure 11.2 *States in the aggregation of an initially uniform distribution of slime molds (each dot represents a cell). [From Bonner, J. T. (1974).* On Development; the biology of form. *fig. 39. Reprinted by permission of Harvard University Press, Cambridge, Mass., fig. 39.]*

4. The rate of degradation of cAMP depends linearly on its concentration.
5. cAMP diffuses passively over the aggregation field.

Of this list, only assumptions 3 and 4 are drastic simplifications.

These assumptions lead to the following set of equations, given here for a one-dimensional domain:

$$\frac{\partial a}{\partial t} = -\frac{\partial}{\partial x}(J_{\text{random}} + J_{\text{chemotactic}}), \tag{1a}$$

$$\frac{\partial c}{\partial t} = -\frac{\partial}{\partial x}(J_{\text{diffusion}}) + \text{sources}, \tag{1b}$$

where

$a(x, t)$ = density of cellular slime mold amoebae per unit area at (x, t),
$c(x, t)$ = concentration of cAMP (per unit area) at (x, t),
J = flux.

By the results of Chapter 9, the appropriate assumptions for chemotactic and for random motion lead to flux terms that can be incorporated into these equations; we then obtain the following:

$$\frac{\partial a}{\partial t} = -\frac{\partial}{\partial x}\left(-\mu \frac{\partial a}{\partial x} + \chi a \frac{\partial c}{\partial x}\right), \tag{2a}$$

$$\frac{\partial c}{\partial t} = -\frac{\partial}{\partial x}\left(-D\frac{\partial c}{\partial}\right) + fa - kc, \tag{2b}$$

where

μ = amoeboid motility,
χ = chemotactic coefficient,
D = diffusion rate of cAMP,
f = rate of cAMP secretion per unit density of amoebae,
k = rate of degradation of cAMP in environment.

The quantities μ, χ, f, and k may in principle depend on cellular densities and chemical concentrations, but for a first step they are assumed to be constant parameters of the system.

We shall study this model in two stages. First we find the simplest solution of the equations, that is, a solution constant in both space and time. This is called the homogeneous steady state. We will next examine its stability properties and thereby address the question of aggregation.

11.2 HOMOGENEOUS STEADY STATES AND INHOMOGENEOUS PERTURBATIONS

A *homogeneous steady state* of a PDE model is a solution that is constant in space and in time. For equations (2) such solutions must then satisfy the following:

$$c(x, t) = \bar{c}, \qquad a(x, t) = \bar{a}, \tag{3a}$$

where

$$\frac{\partial \bar{c}}{\partial t} = \frac{\partial \bar{a}}{\partial t} = 0, \tag{3b}$$

$$\frac{\partial \bar{c}}{\partial x} = \frac{\partial \bar{a}}{\partial x} = 0.$$

Now substitute these into equations (2a,b). Observe that, since all derivatives are zero, one obtains

$$0 = 0,$$
$$0 = 0 + f\bar{a} - k\bar{c},$$

In the homogeneous steady state it must follow that

$$f\bar{a} = k\bar{c}. \tag{4}$$

This means that in every location the amount of cAMP degraded per unit time matches the amount secreted by cells per unit time.

It is of interest to determine whether or not such steady states are stable. As before, we analyze stability properties by considering the effect of small perturbations. However, a somewhat novel feature of the problem to be exploited is its space dependence. In determining whether aggregation of slime molds is likely to begin, we must look at spatially nonuniform (also called *inhomogeneous*) perturbations, and explore whether these are amplified or attenuated.

If an amplification occurs, then a situation close to the spatially uniform steady state will *destabilize*, leading to some new state in which spatial variations predominate. Keller and Segel (1970) identified the *onset of aggregation* with a process of destabilization.

Starting close to $\bar{a}$ and $\bar{c}$ we take our distributions to be

$$a(x, t) = \bar{a} + a'(x, t), \tag{5a}$$
$$c(x, t) = \bar{c} + c'(x, t), \tag{5b}$$

where a' and c' are small. In preparation, we rewrite (2) in the expanded form

$$\frac{\partial a}{\partial t} = \mu \frac{\partial^2 a}{\partial x^2} - \chi\left(\frac{\partial a}{\partial x}\frac{\partial c}{\partial x} + a\frac{\partial^2 c}{\partial x^2}\right), \tag{6a}$$

$$\frac{\partial c}{\partial t} = D\frac{\partial^2 c}{\partial x^2} + fa - kc. \tag{6b}$$

In this form equations (6a,b) contain two nonlinear terms within parentheses. (All other terms contain no multiples or nonlinear functions of the dependent variables.) However, the fact that a' and c' *are small* permits us to neglect the nonlinear terms. To see this, substitute (5a,b) into (6a,b) and expand. Then using the fact that $\bar{a}$ and $\bar{c}$ are constant and uniform we arrive at the following equations:

$$\frac{\partial a'}{\partial t} = \mu \frac{\partial^2 a'}{\partial x^2} - \chi\left(\frac{\partial a'}{\partial x}\frac{\partial c'}{\partial x} + \bar{a}\frac{\partial^2 c'}{\partial x^2} + a'\frac{\partial^2 c'}{\partial x^2}\right), \tag{7a}$$

$$\frac{\partial c'}{\partial t} = D\frac{\partial^2 c'}{\partial x^2} + fa' - kc'. \tag{7b}$$

The terms $(\partial a'/\partial x)(\partial c'/\partial x)$ and $a'\partial^2 c'/\partial x^2$ are quadratic in the perturbations or their derivatives and consequently are of smaller magnitude than other terms, provided a' and c' and their derivatives are small (see problem 1).

We now rewrite the approximate equations:

$$\frac{\partial a'}{\partial t} = \mu\frac{\partial^2 a'}{\partial x^2} - \chi\bar{a}\frac{\partial^2 c'}{\partial x^2}, \tag{8a}$$

$$\frac{\partial c'}{\partial t} = D\frac{\partial^2 c'}{\partial x^2} + fa' - kc'. \tag{8b}$$

Note that they are now *linear* in the quantities a' and c'. Based on a similarity with the diffusion equation discussed in the previous chapter, we shall build solutions to equations (8a,b) from the basic functions $e^{\sigma t}\cos qx$ and $e^{\sigma t}\sin qx$. Without attempting to deal in full generality we restrict our attention to the following possibilities:

$$a'(x, t) = Ae^{\sigma t}\cos qx, \tag{9a}$$

$$c'(x, t) = Ce^{\sigma t}\cos qx, \tag{9b}$$

While this rather special assumption may seem at first sight surprising, it makes sense for several reasons.

1. The functions appearing as factors in equations (9a,b) are related to their own first and second partial derivatives (with respect to time and space respectively). These functions are thus good candidates for solutions to equations such as (8) in which $\partial^2/\partial x^2$ and $\partial/\partial t$ appear. (Indeed, such functions were shown to appear rather naturally in Chapter 9, where we encountered their spatial parts as eigenfunctions of the diffusion operator.)
2. The spatial dependence of $\cos qx$ is that of a function with maxima and minima—precisely descriptive of an aggregation field where there is depletion of cells in some places and accumulation in others.
3. Later we explicitly consider the effect of domain size and boundary conditions on the aggregation process. We saw in Section 9.8 that for impermeable boundaries, the eigenfunction $\cos qx$ (where the *wavenumber* q is suitably defined) is appropriate. This will soon be discussed more fully.
4. The time dependence of (9a,b), $e^{\sigma t}$ would be suitable for either increasing or decreasing perturbations. It is up to the analysis to determine whether $\sigma > 0$ (that is, instability of the uniform state) is compatible with the model.
5. In a given realistic example, $a'(x, t)$ and $c'(x, t)$ might have more complicated spatial forms. There is then a theorem (called the *Fourier theorem*) analogous to that in the Appendix to Chapter 9, which guarantees that the spatial functional form of the perturbations can be expressed as an infinite sum of cosines. (Such an expansion is called a *Fourier cosine series*.) For simplicity, we are merely isolating one component in (9). Since the approximate equations (8a,b) are linear, it is always possible to construct general solutions from linear superpositions of simpler ones.

Pursuing the consequences of assumptions (9) for the perturbations, we substitute (9) into (8) and differentiate. This leads to

$$A\sigma e^{\sigma t}\cos qx = -\mu q^2 A e^{\sigma t}\cos qx + \chi\bar{a}Cq^2 e^{\sigma t}\cos qx, \tag{10a}$$

$$C\sigma e^{\sigma t}\cos qx = -Dq^2 C e^{\sigma t}\cos qx + fAe^{\sigma t}\cos qx - kCe^{\sigma t}\cos qx. \tag{10b}$$

A factor of $e^{\sigma t}\cos qx$ can be cancelled to obtain a pair of equations in A and C:

$$A(\sigma + \mu q^2) - C(\chi\bar{a}q^2) = 0, \tag{11a}$$

$$A(-f) + C(\sigma + Dq^2 + k) = 0. \tag{11b}$$

Thus equations (9a,b) indeed constitute a solution to (8a,b) provided that algebraic equations (11a,b) are satisfied. One trivial way of solving these is to set $A = C = 0$. (This is in fact the unique solution unless the equations are redundant.) But this is not what we want since it means that the perturbations a' and c' are identically zero for all t. To study nonzero perturbations it is essential to have $A \neq 0$ and $C \neq 0$; the only way this can be achieved is by setting the determinant of equations (11a,b) equal to zero:

$$\det\begin{pmatrix} \sigma + \mu q^2 & -\chi\bar{a}q^2 \\ -f & \sigma + Dq^2 + k \end{pmatrix} = 0. \tag{12}$$

The resulting equation for σ is then

$$(\sigma + \mu q^2)(\sigma + Dq^2 + k) - \chi\bar{a}q^2 f = 0, \tag{13}$$

or, after rearranging terms, the quadratic equation in σ:

$$\sigma^2 + \beta\sigma + \gamma = 0, \tag{14a}$$

where

$$\beta = q^2(\mu + D) + k, \tag{14b}$$

$$\gamma = q^2[\mu(Dq^2 + k) - \chi\bar{a}f]. \tag{14c}$$

We can now address the question of whether the growth rate σ of the perturbations can ever have a positive real part (Re $\sigma > 0$). First note that the two possible roots of (14a) are

$$\sigma_{1,2} = \frac{-\beta \pm \sqrt{\beta^2 - 4\gamma}}{2}. \tag{15}$$

From (14b) we observe that β is always positive, so there is always one root whose real part is negative. In order for the second root to have a positive real part it is therefore necessary that the value of γ given by (14c) be *negative* [see problem (1e)]:

Condition for Aggregation of Cellular Slime Molds

$$\mu(Dq^2 + k) < \chi\bar{a}f. \tag{16}$$

(*Note:* This also implies that both σ_1 and σ_2 are real numbers.) Under this condition

we may conclude that the homogeneous cell distribution is unstable to perturbations of the form (9) and that the uniform population will begin to aggregate.

11.3. INTERPRETING THE AGGREGATION CONDITION

We shall now pay closer attention to what is actually implied by inequality (16). To do so, first consider the effect of boundary conditions on the quantity q. Suppose the amoebae are confined to a region with length dimension L; that is, $0 < x < L$. This means that equations (2a,b) and therefore also equations (8a,b) are equipped with the boundary conditions

$$\frac{\partial c}{\partial x} = 0 \qquad \text{at} \qquad x = 0, x = L, \tag{17a}$$

$$\frac{\partial a}{\partial x} = 0 \qquad \text{at} \qquad x = 0, x = L. \tag{17b}$$

As we have seen in Section 9.8 such conditions can only be satisfied provided functions (9a,b) are chosen appropriately. In particular, it is essential that

$$\frac{\partial}{\partial x}(\cos qx) = 0 \qquad \text{at} \qquad x = L,$$

that is, $\sin qL = 0$. This is satisfied only for

$$q = \frac{n\pi}{L} \qquad (n = 0, 1, 2, \ldots), \tag{18}$$

where the nonnegative integer n is called the *mode*. Thus inequality (16) implies that

$$\mu\left[\frac{D}{L^2}(n\pi)^2 + k\right] < \chi\bar{a}f. \tag{19}$$

To satisfy this it is necessary to have one or several of the following conditions met:

1. Values of μ, D, k, and/or n must be small.
2. Values of L must be large.
3. Values of χ, $\bar{a}$, and/or f must be large.

This means that the factors promoting the onset of aggregation (leading to instability) are as follows:

1. Low random motility of the cells and a low rate of degradation of cAMP.
2. Large chemotactic sensitivity, high secretion rate of cAMP, and a high density of amoebae, $\bar{a}$.

Indeed, it has been observed experimentally that the onset of *Dictyostelium* aggregation is accompanied by an increase in chemotactic sensitivity and cAMP production, so it appears that these changes indeed bring about the condition for instability, given by inequality (19), that leads to aggregation.

Several other factors apparently promote aggregation; of particular note is the prediction that large L and small n are favorable for instability. This gives the following somewhat surprising results:

1. Aggregation is favored more highly in larger domains than in smaller ones.
2. The perturbations most likely to be unstable are those with low wavelength. For example, $n = 1$ leads to the smallest possible LHS of inequality (19), all else being equal.

The perturbation whose wavelength is $q = \pi/L$ (that is, where $n = 1$) looks like the function shown in Figure 11.3(a). If this is the most unstable mode, we expect that the aggregation domain should first be roughly bisected, with amoebae moving away from one side of the dish and toward the other. Of course, if the parameter values gradually shift so that inequality (19) is also satisfied for $n = 2$, one can expect further subdivision of the domain into smaller *aggregation domains*. Biologists were at one time puzzled about the fact that the size of aggregation domains is not proportional to the density of amoebae $\bar{a}$. This result, too, is explained by inequality (19). (See problem 4.)

From this analysis one gains evidence for Segel's (1980) statement that even relatively simple interactions can have consequences that are not predictable based only on intuition or biological experience. With the hindsight that mathematical analysis gives, Keller and Segel (1970) were able to explain the counterintuitive aspects of the results as follows:

1. The forces of diffusion act most efficiently to smooth large gradients on small length scales. For this reason, in a large dish the long-range variation in cAMP concentrations and in cell densities has a greater chance of being self-reinforced before being obliterated by diffusion.
2. Similarly, the lower wavelengths present locally shallower gradients and are less prone to being effaced by diffusion and random motility.

Suggestions for Further Study or Independent Projects on Cellular Slime Molds

1. *The prespore-prestalk ratio.* See Bonner (1967, 1974) for surveys of older papers and a summary of the observed phenomena. For a more recent review of modeling efforts consult MacWillians and Bonner (1979) and Williams et al. (1981).
2. *cAMP activity and secretion in* D. discoideum. The substance cAMP can be secreted in an excitable or an oscillatory response as well as constant steady levels. In a series of models, Segel and Goldbetter outline the possible underlying molecular events. See Figure 8.16 and Segel (1984), Goldbetter and Segel (1980), and Devreotes and Steck (1979).
3. *Later developmental stages (shape of the aggregate).* See Rubinow et al. (1981).
4. *Locomotion in the slug.* See Odell and Bonner (1981).

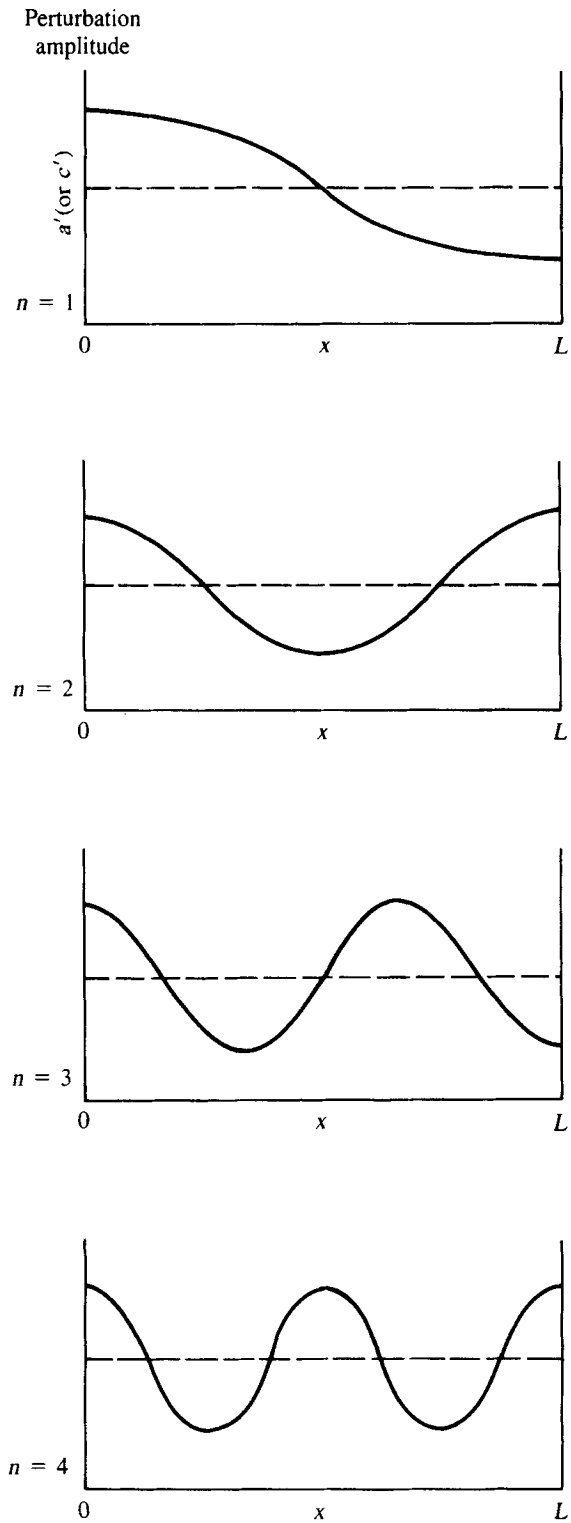

Figure 11.3 *Perturbations* a' *or* c' *of the homogeneous steady state,* $\bar{a}$ *(or* $\bar{c}$*). When a finite one-dimensional domain has imposed boundary conditions, there are restrictions on the wavenumber* q *of permissible perturbations. For example, no-flux boundaries imply that* $\partial(\cos qx)/\partial x = 0$ *at* $x = 0$ *and* $x = L$*. This can only be satisfied for* $q = n\pi/L$*, where* n *is an integer. Examples of the cases where* $n = 1, 2, 3$ *and* 4 *are shown here. The amplitudes have been exaggerated; we can only address the evolution of small-amplitude perturbations. Dotted lines represent a homogeneous steady state of equations (2a,b).*

While it may be said that developmental biologists have to some extent resisted the intrusion of mathematics, the Keller-Segel model has become a classic in this field and is now frequently quoted in biological references. Many other aspects of the differentiation of cellular slime molds are equally, if not more, amazing than the aggregation phase. The topic continues to attract the most refined experimental and theoretical efforts.

11.4. A CHEMICAL BASIS FOR MORPHOGENESIS

Morphogenesis describes the development of shape, pattern, or form in an organism. The processes that underly morphogenesis are rather complex, spanning subcellular to multicellular levels within the individual. They have been studied empirically and theoretically for over a century. Among the first to devote considerable attention to the topic was D'Arcy Thompson, whose eclectic and imaginative book *On Growth and Form* could be considered as one of the first works on theoretical biology. Thompson emphasized the parallels between physical, inorganic, and geometric concepts and the shapes of a variety of plant and animal structures.

Some 35 years ago the theoretical study of morphogenesis received new impetus from a discovery made by a young British mathematician, Alan Turing. In a startling paper dated 1952, Turing exposed a previously little-known physical result that foretold the potential of diffusion to lead to "chemical morphogenesis."

From our daily experience most of us intuitively associate diffusion with a smoothing and homogenizing influence that eliminates chemical gradients and leads to uniform spatial distributions. It comes as some surprise, then, to be told that diffusion can have an opposite effect, engendering chemical gradients and fostering nonuniform chemical "patterns." Indeed, this is what the theory predicts. The following sections demonstrate the mathematical basis for this claim and outline applications of the idea to morphogenesis.

The key elements necessary for chemical pattern formation are:

1. Two or more chemical species.
2. Different rates of diffusion for the participants.
3. Chemical interactions (to be more fully specified shortly).

An appropriate combination of these factors can result in chemical patterns that arise as a destabilization of a uniform chemical distribution.

Turing recognized the implications of his result to biological morphogenesis. He suggested that during stages in the development of an organism, chemical constituents generate a *prepattern* that is later interpreted as a signal for cellular differentiation. Since his paper, chemical substances that play a role in cellular differentiation have been given the general label *morphogen*.

The steps given in this section are aimed at exposing the basic idea on which the Turing (1952) theory is built. To deal in specific terms we consider a set of *two* chemicals that diffuse and interact. For simplicity, a one-dimensional domain is con-

sidered, although it is later shown that the conclusions hold in higher dimensions as well. See Segel and Jackson (1972) for the source of this method.

Let

$$C_1 = C_1(x, t), \qquad C_2 = C_2(x, t),$$

be the concentrations of chemicals 1 and 2, and let

$R_1(C_1, C_2)$ = rate of production of C_1,
$R_2(C_1, C_2)$ = rate of production of C_2,
D_1 = diffusion coefficient of chemical 1,
D_2 = diffusion coefficient of chemical 2.

The quantities R_1 and R_2 (*kinetic terms*) generally depend on concentrations of the participating molecules. By previous remarks we know that a set of equations for C_1 and C_2 consists of the following:

$$\frac{\partial C_1}{\partial t} = R_1(C_1, C_2) + D_1 \frac{\partial^2 C_1}{\partial x_2}, \tag{20a}$$

$$\frac{\partial C_2}{\partial t} = R_2(C_1, C_2) + D_2 \frac{\partial^2 C_2}{\partial x^2}. \tag{20b}$$

To underscore the role of diffusion in pattern formation we assume that in absence of its effects (when solutions are well mixed) the chemical system has some positive spatially uniform steady state, $(\overline{C}_1, \overline{C}_2)$. By definition this means that

$$\frac{\partial \overline{C}_i}{\partial t} = 0, \tag{21a}$$

$$(i = 1, 2).$$

$$\frac{\partial^2 \overline{C}_i}{\partial x^2} = 0. \tag{21b}$$

We therefore conclude that

$$R_1(\overline{C}_1, \overline{C}_2) = 0, \tag{22a}$$

$$R_2(\overline{C}_1, \overline{C}_2) = 0. \tag{22b}$$

As in Section 11.2 we now examine the effects of small *inhomogeneous perturbations of this steady state*. We are specifically interested in those perturbations that are amplified by the combined forces of reaction and diffusion in equations (1) and (2). When such perturbations are introduced, the uniform distributions $\overline{C}_1$ and $\overline{C}_2$ are upset.

Let

$$C_1'(x, t) = C_1(x, t) - \overline{C}_1, \tag{23a}$$

$$C_2'(x, t) = C_2(x, t) - \overline{C}_2, \tag{23b}$$

be small nonhomogeneous perturbations of the uniform steady state. Provided these are sufficiently small, it is again possible to linearize equations (20a,b) about the homogeneous steady state. Recall that this can be achieved by writing Taylor-series expansions for $R_1(\overline{C}_1, \overline{C}_2)$ and $R_2(\overline{C}_1, \overline{C}_2)$ about the values $\overline{C}_1$, and $\overline{C}_2$ and retaining the

linear contributions (see problem 9). We then obtain the linearized version of equations (20a,b):

$$\frac{\partial C_1'}{\partial t} = a_{11}C_1' + a_{12}C_2' + D_1\frac{\partial^2 C_1'}{\partial x^2}, \tag{24a}$$

$$\frac{\partial C_2'}{\partial t} = a_{21}C_1' + a_{22}C_2' + D_2\frac{\partial^2 C_2'}{\partial x^2}, \tag{24b}$$

where

$$\begin{aligned} a_{11} &= \left.\frac{\partial R_1}{\partial C_1}\right|_{\bar{c}_1,\bar{c}_2}, \qquad a_{12} = \left.\frac{\partial R_1}{\partial C_2}\right|_{\bar{c}_1,\bar{c}_2}, \\ a_{21} &= \left.\frac{\partial R_2}{\partial C_1}\right|_{\bar{c}_1,\bar{c}_2}, \qquad a_{22} = \left.\frac{\partial R_2}{\partial C_2}\right|_{\bar{c}_1,\bar{c}_2}, \end{aligned} \tag{25}$$

and C_1' and C_2' are perturbations from $\bar{C}_1$ and $\bar{C}_2$. For convenience, these equations can be written in the shorthand matrix form:

$$\mathbf{C}_t' = \mathbf{M}\mathbf{C}' + \mathbf{D}\mathbf{C}_{xx}', \tag{26a}$$

where

$$\mathbf{C}' = \begin{pmatrix} C_1'(x,t) \\ C_2'(x,t) \end{pmatrix} = \begin{pmatrix} C_1(x,t) - \bar{C}_1 \\ C_2(x,t) - \bar{C}_2 \end{pmatrix} \tag{26b}$$

$$\mathbf{M} = \begin{pmatrix} a_{11} & a_{12} \\ a_{21} & a_{22} \end{pmatrix}, \tag{26c}$$

$$\mathbf{D} = \begin{pmatrix} D_1 & 0 \\ 0 & D_2 \end{pmatrix}. \tag{26d}$$

The resulting system of equations is linear. It can be solved by various methods, including separation of variables. One set of possible solutions is

$$\mathbf{C}' = \begin{pmatrix} C_1' \\ C_2' \end{pmatrix} = \begin{pmatrix} \alpha_1 \\ \alpha_2 \end{pmatrix} \cos qx\, e^{\sigma t}. \tag{27}$$

(See problem 9.) While this is a special form, considerations identical to those of Section 11.2 are again viewed as sufficient justification for restricting analysis to this set of solutions.

By substituting perturbations (27) into equations (24) or (26) we obtain

$$\begin{aligned} \alpha_1\sigma &= a_{11}\alpha_1 + a_{12}\alpha_2 - D_1q^2\alpha_1, \\ \alpha_2\sigma &= a_{21}\alpha_1 + a_{22}\alpha_2 - D_2q^2\alpha_2. \end{aligned}$$

While the quantities α_1, α_2, q, and σ are *a priori* unknown to us, we are interested specifically in the situation in which small perturbations *grow with time*. Rewriting these as linear equations in α_1 and α_2, we obtain

$$\alpha_1(\sigma - a_{11} + D_1q^2) + \alpha_2(-a_{12}) = 0, \tag{28a}$$

$$\alpha_1(-a_{21}) + (\sigma - a_{22} + D_2q^2)\alpha_2 = 0, \tag{28b}$$

As in Section 11.2, we arrive at a set of algebraic equations in the perturbation amplitudes α_1 and α_2. Since the RHS is (0, 0), one solution is always $\alpha_1 = \alpha_2 = 0$.

This is dismissed as a trivial case; that is, perturbations are absent altogether for all t. But a nontrivial solution can only exist if the determinant of the coefficients appearing in equations (28a,b) is zero. It is thus essential that

$$\det \begin{pmatrix} \sigma - a_{11} + D_1 q^2 & -a_{12} \\ -a_{21} & \sigma - a_{22} + D_2 q^2 \end{pmatrix} = 0. \tag{29}$$

This leads to the following equation:

$$(\sigma - a_{11} + D_1 q^2)(\sigma - a_{22} + D_2 q^2) - a_{12}a_{21} = 0,$$

or

$$\sigma^2 + \sigma(-a_{22} + D_2 q^2 - a_{11} + D_1 q^2) + [(a_{11} - D_1 q^2)(a_{22} - D_2 q^2) - a_{12}a_{21}] = 0. \tag{30}$$

Equation (30) is called the eigenvalue or the characteristic equation.

Our next goal is to determine whether for some q, the eigenvalue σ can have a positive real part, in other words, whether perturbations of particular "waviness" can cause instability to occur.

11.5. CONDITIONS FOR DIFFUSIVE INSTABILITY

As in previous analysis (of both ordinary and partial differential equations) the characteristic equation (30) will now be used to determine whether growing perturbations are possible. From equation (27) it is clear that the eigenvalue σ (the growth rate of the perturbations) should have a positive real part: Re $\sigma > 0$.

To concentrate solely on diffusion as a destabilizing influence we now incorporate the assumption that *in the absence of diffusion the reaction mixture is stable*. This implies that by setting $D_1 = D_2 = 0$ in equations (24) or in equation (30) one obtains only negative values of Re σ (consistent with stability). Eliminating D_1 and D_2 from equation (30) leads to

$$\sigma^2 - \sigma(a_{11} + a_{22}) + (a_{11}a_{22} - a_{12}a_{21}) = 0. \tag{31}$$

This quadratic equation is identical (save for the renaming of quantities) to the characteristic equation of the system of 2 ODEs obtained by omitting the diffusion terms in equations (20a,b). The conditions under which Re σ is negative are thus identical to stability conditions derived in Section 4.9:

Conditions for Stability of the Chemicals in the Absence of Diffusion

1. $a_{11} + a_{22} < 0,$ *(32a)*

2. $a_{11}a_{22} - a_{12}a_{21} > 0,$ *(32b)*

Strictly speaking, the second of these is required in the case where σ is real.

To appreciate how diffusion can act as a destabilizing influence, we consider analogous conditions obtained from equation (30) where $D_1, D_2 \neq 0$. By violating

any *one* of these, a regime of instability would be created. The inequalities are as follows:

1. $$(a_{11} + a_{22} - D_2q^2 - D_1q^2) < 0, \tag{33a}$$

2. $$[(a_{11} - D_1q^2)(a_{22} - D_2q^2) - a_{12}a_{21}] > 0. \tag{33b}$$

Violation of either (1) or (2) leads to diffusive instability.

Because D_1 and D_2 and q^2 are positive quantities, it is clear that condition 33(a) always holds whenever 32(a) is true. The only other possibility then is that 33(b) may be reversed for certain parameter values. To study this more closely, we represent the LHS of 33(b) by H. We require that

$$H < 0. \tag{34}$$

By expanding the expression, H is found to be

$$H = D_1D_2(q^2)^2 - (D_1a_{22} + D_2a_{11})(q^2) + (a_{11}a_{22} - a_{12}a_{21}). \tag{35}$$

This expression seems complicated at first glance, but it can be understood in a straightforward way. Let us consider H as a function of q^2 and note that equation (35) is then simply a quadratic expression (with coefficients that depend on the a_{ij} and D_i).

Since the coefficient of $(q^2)^2$, D_1D_2, is positive, the graph of $H(q^2)$ is a parabola opening upwards (see Figure 11.4). The function thus has a minimum for some value of q^2. By simple calculus the value of this minimum can be determined. It is found to be

$$q^2_{\min} = \frac{1}{2}\left(\frac{a_{22}}{D_2} + \frac{a_{11}}{D_1}\right). \tag{36a}$$

(See problem 10.) Clearly, in order to satisfy (34) a minimal condition is that $H(q^2_{\min})$ should be negative:

$$H(q^2_{\min}) < 0, \tag{36b}$$

In problem 10 the reader is asked to evaluate $H(q^2_{\min})$ and thus demonstrate that (36) implies that

$$(a_{11}a_{22} - a_{12}a_{21}) - \frac{1}{4}\left(\frac{D_1a_{22} + D_2a_{11}}{D_1D_2}\right) < 0. \tag{37}$$

A more common way of writing this expression, after some rearranging and incorporating (32b), is as follows:

$$(a_{11}D_2 + a_{22}D_1) > 2\sqrt{D_1D_2}(a_{11}a_{22} - a_{12}a_{21})^{1/2} > 0. \tag{38}$$

(See problem 10.) When (38) is satisfied, $H(q^2_{\min})$ will be negative, so that for wavenumbers close to $q^2_{\min}$ the growth rate of perturbations σ can be positive. This in turn implies that diffusive instability to small perturbations of the form (27) will take place. Following is a summary of the key steps leading to this result.

Summary of Procedure for Deriving Conditions for Diffusive Instability

1. Equations:

$$(C_i)_t = D_i(C_i)_{xx} + R_i(C_1, C_2) \qquad (i = 1, 2).$$

2. Assume a spatially uniform steady state $(\bar{C}_1, \bar{C}_2)$.
3. Assume perturbations $C_i'(x, t) = \alpha_i e^{\sigma t} \cos qx$, where

   σ = growth rate in time,

   α_i = amplitude at $t = 0$,

   q = wavenumber ($\sim 2\pi$/distance between peaks).

4. Find set of algebraic equations (28a,b) for α_i, σ, and q that must have zero determinant for nontrivial perturbations.
5. Obtain a characteristic equation (30) for σ from step 4. Then next steps are conditions that guarantee $\mathrm{Re}(\sigma) > 0$.
6. Assume conditions (32a,b) to insure stability of chemical mixture when $D_i = 0$.
7. Violate (33b) for instability of the system when $D_i \neq 0$. [It is impossible to violate (33a)].
8. Find a quadratic expression $H(q^2)$ that must be negative to violate (33b).
9. Constrain the minimal value of this expression, $H(q^2_{\min})$ to be negative, thus obtaining (37).
10. Use (32b) to rewrite the condition as (38).

The three conditions for diffusive instability are then as follows:

Necessary and Sufficient Conditions for Diffusive Instabilty

1. $a_{11} + a_{22} < 0,$ *(32a)*
2. $a_{11}a_{22} - a_{12}a_{21} > 0,$ *(32b)*
3. $a_{11}D_2 + a_{22}D_1 > 2\sqrt{D_1D_2}(a_{11}a_{22} - a_{12}a_{21})^{1/2} > 0.$ *(38)*

It can be shown by simple rearrangement that the last of these may also be written in the following dimensionless form:

3. $\beta^{1/2} + \alpha\beta^{-1/2} > 2(\alpha - \epsilon)^{1/2} > 0$, where *(39)*

$$\beta = \frac{D_2}{D_1}, \qquad \alpha = \frac{a_{22}}{a_{11}} \quad (a_{11} > 0), \qquad \epsilon = \frac{a_{12}a_{21}}{a_{11}^2}.$$

(See problem 10.) We thus see that the condition for diffusive instability depends on dimensionless ratios of diffusion constants (and of kinetic terms) and not on any absolute magnitude.

In the next section we follow a physical interpretation of conditions (38) proposed by Segel and Jackson (1972).

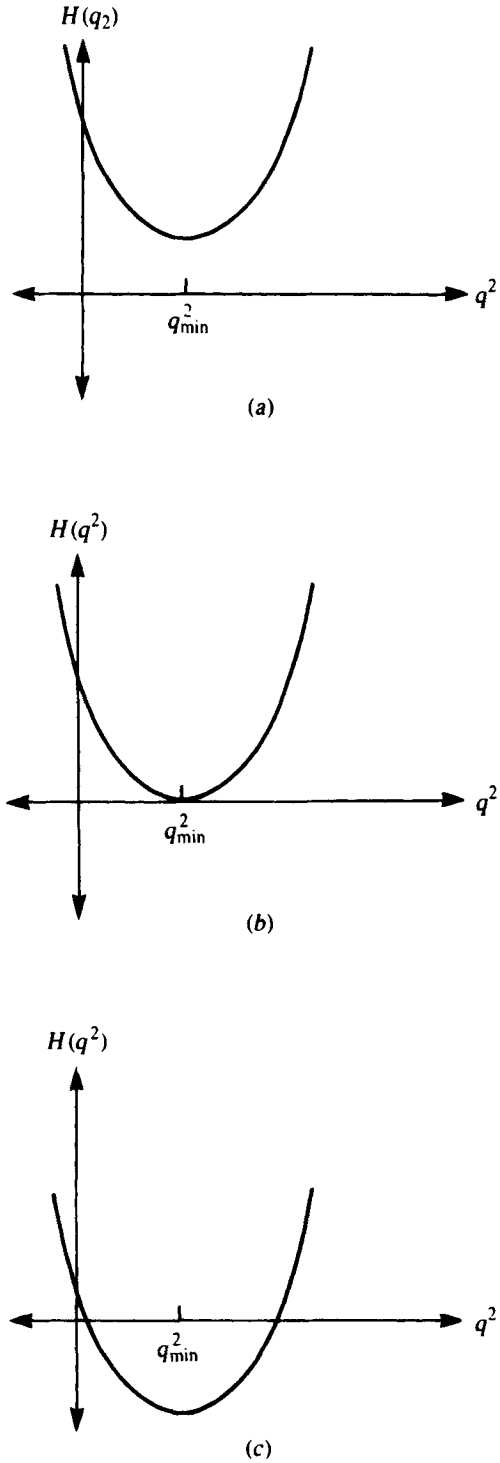

Figure 11.4 *This sequence illustrates how the graph of* $H(q^2)$ *given by equation (35) might change as a parameter variation causes the onset of diffusive instability. (a)* H *is positive for all* q^2. *(b)* $H = 0$ *at* q^2_{min}, *which would then be the wavenumber of destabilizing perturbations. (c) A whole range of* q^2 *values makes* H *negative. Any one of these wavenumbers would lead to diffusive instability.*

11.6 A PHYSICAL EXPLANATION

Turing's (1952) paper was followed a decade later by generalizations and extensions of the theory. The Brussels school, including G. Nicolis, I. Prigogine, and coworkers, based most of their ideas on mathematical and thermodynamic arguments, many of which would be inaccessible to most readers [see, for example, Nicolis and Prigogine, (1977)]. Segel and Jackson (1972) were apparently the first team to derive necessary and sufficient conditions for diffusive instability [equations (32a,b) and (38)] and then explain the meaning in an elegantly simple way. The logical progression of steps leading to their conclusions is reproduced here.

1. By condition (32a) at least one of the two coefficients, a_{11} or a_{22}, is negative. Suppose a_{22} is negative.

Interpretation: $\partial R_2/\partial c_2 < 0$; chemical 2 inhibits its own rate of formation. We shall call this substance an *inhibitor*.

2. From condition (38), $a_{11}D_2 + a_{22}D_1 > 0$, so clearly a_{11} and a_{22} cannot both be zero. Therefore a_{11} must be positive.

Interpretation: $\partial R_1/\partial c_1 > 0$; chemical 1 promotes or activates its own formation. This chemical species is called an *activator*.

3. Steps 1 and 2 together imply that

$$a_{11}a_{22} < 0. \tag{40}$$

4. From step 3 it follows that the inequality (32b) ($a_{11}a_{22} - a_{12}a_{21} > 0$) can only be met if

$$a_{12}a_{21} < 0. \tag{41}$$

This means that one of the two quantities, a_{12} or a_{21}, but not both, is negative. There are then two possibilities, each giving a distinct sign pattern to the Jacobian matrix **M** [equation (26c)]:

1. *Activator-inhibitor:*

$$a_{12} < 0, \qquad a_{21} > 0 \qquad \mathbf{M} = \begin{pmatrix} + & - \\ + & - \end{pmatrix}$$

2. *Positive feedback* (also called *substrate depletion*).

$$a_{12} > 0, \qquad a_{21} < 0 \qquad \mathbf{M} = \begin{pmatrix} + & + \\ - & - \end{pmatrix}.$$

These are precisely the two cases that were explored in connection with pairs of chemically interacting substances in Section 7.8. Recall that these were called,

partly for historic reasons, an activator-inhibitor and a positive-feedback system respectively.

By Segel and Jackson's reasoning, two chemical species that have the attribute of diffusive instability can only fall under one of these two classes. Moreover, in order for the chemical system to be stable when diffusion is absent (for example, in a well-stirred solution), a steady state of the (spatially) homogeneous system

$$\frac{dC_i}{dt} = R_i(C_1, C_2), \tag{42}$$

must be stable.

Necessary and sufficient geometric conditions for stability of such steady states were derived in Section 7.8. There we discovered that the nullclines of the present system must satisfy certain intersection properties (see Figure 7.10). If a given set of reactants has such qualitative geometry in the C_1C_2 phase plane, it makes a strong candidate for diffusive instability *provided that the condition given by (38) is also satisfied*. (Please note that axes in Figure 7.10(b) should be renamed in case 2 since the roles of the two chemicals have been permuted in the positive-feedback case.)

We continue to draw further conclusions about the two chemicals:

5. Dividing (38) through by D_2 leads to the following:

$$a_{11} + a_{22}\frac{D_1}{D_2} > 0. \tag{43}$$

This condition is met only if $D_1 \neq D_2$ because otherwise the inequality $a_{11} + a_{22}1 < 0$ contradicts (32a).

Interpretation: The diffusion coefficients of chemicals 1 and 2 must be dissimilar for diffusive instability to occur.

6. In both cases 1 and 2, signs of a_{11} and a_{22} are opposite.

Now define

$$\tau_1 = 1/|a_{11}|, \tag{44a}$$

$$\tau_2 = 1/|a_{22}|, \tag{44b}$$

where τ_1 and τ_2 are time constants associated with activation and inhibition. One can deduce from inequality (38) that

$$D_1\tau_1 < D_2\tau_2 \tag{45}$$

(see problem 11). Based on dimensional considerations and the discussion in Chapter 9, the ratios in (45) have units of area or, more precisely, mean square displacement during the doubling time of the activator or the half-life of the inhibitor (see problem 11). The quantities $\sqrt{D_1\tau_1}$ and $\sqrt{D_2\tau_2}$ are referred to as the *ranges* of activation

or inhibition. They represent a unit of length over which a peak concentration of chemical tends to exert its effect. Thus inequality (45) can be restated in word as follows:

> The range of inhibition $\sqrt{D_2\tau_2}$ is larger than the range of activation $\sqrt{D_1\tau_1}$.

Based on these conclusions, it can also be shown that $D_2 > D_1$ (problem 11). Together these observations give us the following picture of how diffusive instability is caused. Consider in particular the activator-inhibitor case. As a result of random perturbations, a small peak concentration of the activator is created at some location. This causes an enhanced local production of the inhibitor that, were it not for diffusion, would halt and reverse the process. However, the inhibitor diffuses away more rapidly than the activator ($D_2 > D_1$), so it cannot control the local activator production; thus the peak will grow). Now the region surrounding the initial peak will contain sufficient levels of inhibition to prevent further peaks of activation. This leads to the typical peak areas characterized by the expression D_2/τ_2 in inequality (45). (Case 2 is left as an exercise for the reader.)

The idea described in the previous paragraph is actually a special case of a much more general and ubiquitous pattern-forming mechanism called *lateral inhibition*. Briefly, positive reinforcement on a local scale together with a longer range of inhibition is universally applied in a variety of pattern-generating mechanisms, many of which are not driven by diffusion per se. Several examples for further study are given in the concluding sections of the chapter.

Can any other statements be made regarding the actual chemical patterns that are produced by these reaction-diffusion schemes? Here some care must be taken; our analysis will work *only* as long as the perturbations are sufficiently small to render the linear approximation of equations (24a,b) a valid representation of the truly nonlinear system of equations (20a,b). When the perturbations have been amplified beyond a small size, the analysis is no longer adequate. As in previous examples, *linear stability theory* applies only to states *close* to a steady state.

To extract even more information from our analysis we now consider how parameter variations bring about the onset of diffusive instability and what might be anticipated as a natural progression of events. It is well known that, as in the example of cellular slime molds, the process of development is often accompanied by gradual variations in characteristics of cells or tissues that could be depicted by key parameters. Such changes may stem from enhanced enzyme activity, increased affinity of reactions, or changes in cell–cell contacts (*gap junctions*) that permit intercellular communication.

It is often the case that dependence on cellular parameters enter into expressions such as (38) in nontrivial ways since the coefficients a_{ij} may depend in a complicated way on any given coefficient in the original nonlinear equations. Nevertheless, to take a simplified view, consider the following plausible (but not necessarily exclusive) progression brought about as a single parameter Γ varies through a *critical bifurcation value* Γ^*:

1. For $\Gamma < \Gamma^*$, diffusive instability is not possible. The parabola $H(q^2)$ is positive for all wavelengths q. No perturbations of any wavelength can lead to pattern formation.
2. For $\Gamma = \Gamma^*$, $H(q_{\min}^2) = 0$. This is the threshold situation. Just beyond it lies the realm of diffusive instability; that is, for slightly larger values of Γ, H is negative but only for values of q^2 very close to $q_{\min}^2$. Only perturbations whose wavenumber is $q_{\min}$ will be amplified and expressed in the final patterns.
3. For $\Gamma > \Gamma^*$, $H(q^2) < 0$ for a whole range of q values:

$$q_{\min}^2 - \Delta \leq q^2 \leq q_{\min}^2 + \Delta.$$

Any perturbation whose wavenumber falls within this range will be amplified.

Situation 2 is often called the *onset of diffusive instability*. At this critical point one would expect patterns with a typical spacing between chemical concentration peaks $\hat{d}$, where

$$\hat{d} = \frac{2\pi}{q_{\min}}. \tag{46}$$

Summary of Two-Species Chemical Interactions Leading to Pattern Formation

Necessary conditions

1. The system must have a nontrivial spatially uniform steady state $\bar{S}$.
2. The pair must interact as an activator-inhibitor *or* a positive feedback system (in the sense that the sign pattern of the Jacobian of the system at $\bar{S}$ is the same as one of the cases given in this section).
3. (a) The steady state $\bar{S}$ should be *stable* in the well-mixed system. This is *equivalent* to the following:
   (b) The configuration of nullclines $R_1(C_1, C_2) = 0$ and $R_2(C_1, C_2) = 0$ at their nontrivial intersection should be of the type shown in Figures 7.10(*a* or *b*).
4. The rate of diffusion of the inhibitor (in case 1) or of the substance receiving negative feedback (in case 2) must be larger than that of the other activating substance.

Necessary and sufficient conditions

5. (a) Conditions (32a,b) and (38) should be satisfied, or
   (b) All necessary conditions 1 through 4 hold and, in addition,

$$\frac{a_{22}}{D_2} + \frac{a_{11}}{D_1} > 0.$$

This is equivalent to the statement that the *range of activation is smaller than the range of inhibition*.

Beyond the onset of diffusive instability the situation becomes somewhat more complicated. A whole range of possible wavenumbers can have a destabilizing effect. In general, perturbations might consist of many modes superimposed on one another, for example,

$$\begin{pmatrix} C_1' \\ C_2' \end{pmatrix} = \sum_{k=1}^{\infty} \begin{pmatrix} \alpha_{1k} \\ \alpha_{2k} \end{pmatrix} e^{\sigma_k t} \cos q_k x. \tag{47}$$

Once nonlinear effects become important, different modes may compete for dominance. Those that initially grow fastest may gain an advantage over others. It is possible to solve equation (30) for the growth rate σ_k associated with a given wavenumber q_k and thus determine the maximum possible growth rate. See Segel (1984) and problem 12. Beyond this, little more can be said analytically about the final patterns that diffusive instability creates. Further understanding requires considerably more elaborate *nonlinear* analysis and is beyond our scope.

An alternative to further analytical techniques is numerical simulation. In Section 11.8 we describe several references that present results based solely on computer-aided numerical solutions.

11.7 EXTENSION TO HIGHER DIMENSIONS AND FINITE DOMAINS

The analysis of reaction-diffusion systems has thus far been restricted to infinite one-dimensional domains. We now extend it to higher dimensions and indicate what new features arise when the system is confined to a bounded domain, for example, a rectangle in the plane.

Consider the following general reaction-diffusion system:

$$\frac{\partial C_1}{\partial t} = R_1(C_1, C_2) + D_1 \nabla^2 C_1, \tag{48a}$$

$$\frac{\partial C_2}{\partial t} = R_2(C_1, C_2) + D_2 \nabla^2 C_2, \tag{48b}$$

with homogeneous steady state $(\bar{C}_1, \bar{C}_2)$.

It is a straightforward matter to carry out the linearization of (48). Results are similar to (24) where $\nabla^2 C_i$ replaces $(\partial^2 C_i/\partial x^2)$. The form of perturbations to be used in testing stability is slightly different since variation in both spatial dimensions may occur. In problem 14 the reader is asked to verify the following set of possible solutions to a *two*-dimensional linear system:

$$C_i'(x, y; t) = \alpha_i e^{\sigma t} \cos q_1 x \cos q_2 y \tag{49}$$

where q_1 and q_2 are the wavenumbers for variations in the x and y directions respectively.

Now consider a finite rectangular domain of size $L_x \times L_y$. By way of example, suppose that the boundaries are impermeable (that is, no flux boundary conditions apply). Then

$$\frac{\partial C_i'}{\partial x} = 0 \qquad \text{at} \qquad x = 0, L_x, \tag{50a}$$

$$\frac{\partial C_i'}{\partial y} = 0 \qquad \text{at} \qquad y = 0, L_y,. \tag{50b}$$

To satisfy these additional constraints, q_i can only take on one of a discrete set of values:

$$q_1 = \frac{m\pi}{L_x} \qquad (m = 0, 1, \ldots), \tag{51a}$$

$$q_2 = \frac{n\pi}{L_y} \qquad (n = 0, 1, \ldots). \tag{51b}$$

(See problem 19.)

Define

$$Q^2 = q_1^2 + q_2^2. \tag{52}$$

Then it may be shown that one obtains a set of algebraic equations for the perturbation amplitudes α_i identical to (28) where Q^2 replaces q^2. This leads to an identical condition for diffusive instability after a procedure analogous to that of Section 11.5 (The dimensionality and geometry of the region have no influence on the stability condition.) However, one finds that the most destabilizing perturbations are those for which

$$Q^2 = Q_{\min}^2 = \frac{1}{2}\left(\frac{a_{22}}{D_2} + \frac{a_{11}}{D_1}\right). \tag{53}$$

Thus, at the onset of diffusive instability the waves that are amplified are those that satisfy

$$Q^2 = \pi^2\left(\frac{m^2}{L_x^2} + \frac{n^2}{L_y^2}\right) = \frac{1}{2}\left(\frac{a_{11}}{D_1} + \frac{a_{22}}{D_2}\right). \tag{54}$$

As we shall soon see, this implies that the wavenumbers q_1 and q_2 are interdependent. For a given *value* of the RHS of equation (53), increasing q_1 must mean decreasing q_2. To examine the effects of geometry and chemistry on the most excitable waves, it proves convenient to use the following dimensionless quantities:

$$\gamma = \frac{L_y}{L_x}, \qquad \beta = \frac{D_2}{D_1}, \qquad \alpha = \frac{a_{22}}{a_{11}}. \tag{55}$$

Then equation (54) can be rewritten in the following dimensionless form:

$$m^2 + \frac{n^2}{\gamma^2} = \frac{L^2 a}{2\pi^2 D}\left(1 + \frac{\alpha}{\beta}\right) \equiv E^2, \tag{56}$$

where we have written $L = L_x$, $a = a_{11}$, and $D = D_1$ for a more convenient notation. Ratios appearing in (56) bear important physical interpretations:

$L^2 \simeq$ area characteristic of the domain ($\equiv$ area of domain if $\gamma = 1$),

$\frac{D}{a} \simeq$ area of range of inhibitor,

$\frac{L^2 a}{D} \simeq$ ratio of area characterizing domain to range of inhibition,

$$\frac{\alpha}{\beta} = \frac{a_{22}/a_{11}}{D_2/D_1} = \frac{D_1/a_{11}}{D_2/a_{22}}$$

$=$ ratio of range of inhibition to range of activation.

Thus the quantity E^2, defined by the RHS of equation (56), stands for

$$E^2 = \frac{\text{area of domain}}{\text{range of inhibition}}\left(1 + \frac{\text{range of inhibition}}{\text{range of activation}}\right).$$

Note that, by (54), $E^2 = Q^2 L_x^2/\pi^2$.

In the following example of parameter variations it will be assumed that α and β [and ϵ appearing in (39)] are held fixed so that condition (39) is just satisfied. Thus we consider a system at the *onset* of diffusive instability when *only* the modes satisfying (54) or alternatively (56) lead to the formation of patterns. From equation (56) it can be seen that the value of E^2 can be changed even though α and β might be held constant. For example, this can be done by

1. Increasing the diffusion rates D_1 and D_2 of both chemicals but keeping $\beta = D_2/D_1$ fixed.
2. Altering all the chemical reaction rates a_{ij} while keeping $\alpha = a_{22}/a_{11}$ and $\epsilon = a_{12}a_{21}/a_{11}^2$ fixed.
3. Increasing or decreasing the domain size L.

The effect of any such parameter variation is that the relative ratios of the domain size and the chemical range size will change. As such changes occur, the value of E^2 changes. One then expects abrupt transitions in the values of m and n that satisfy (56).

In the following example we take $\gamma = 2$ for illustrative purposes. We compute the expression

$$E^2 = m^2 + \frac{n^2}{\gamma^2} \qquad \begin{cases} m = 0, 1, 2, \ldots . \\ n = 0, 1, 2, \ldots , \end{cases}$$

and then rank the pairs of integers (m, n) in order of increasing values of E^2 (see Figure 11.5). The succession of modes thus generated might arise from any one of the above parameter variations (as long as E^2 is thereby made to vary gradually and monotonically). A different value of γ would lead to a somewhat different sequence of modes. Some of the chemical patterns corresponding to such modes are then displayed schematically in Figure 11.6.

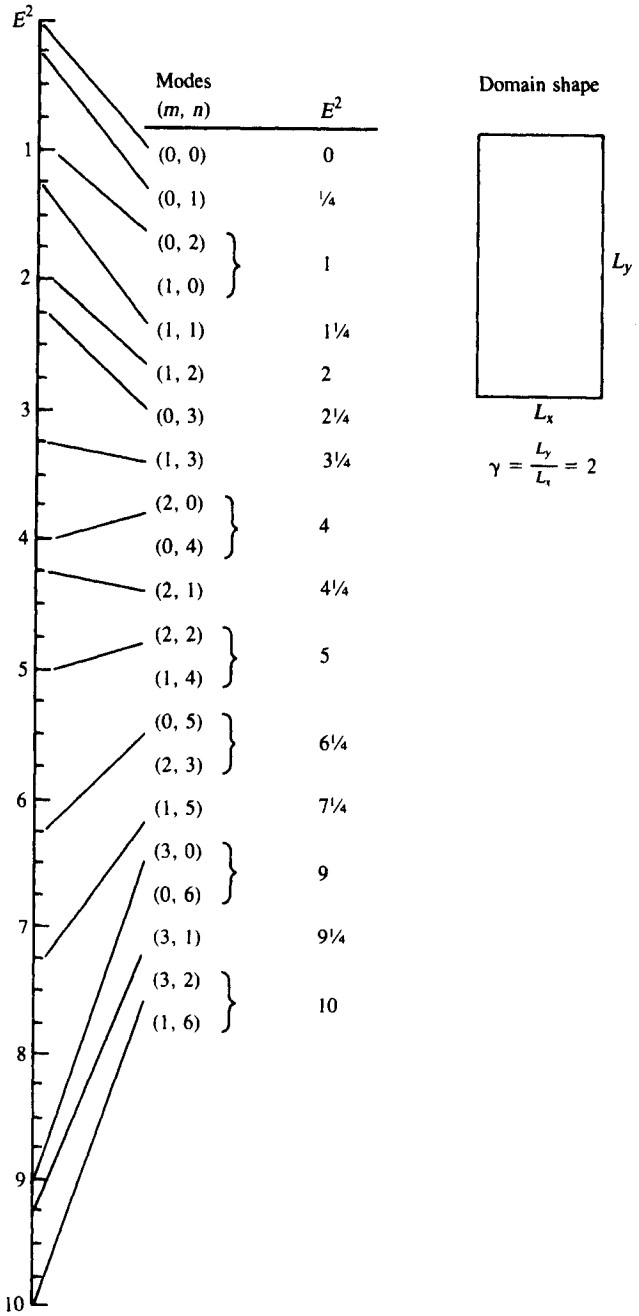

Figure 11.5 *In a two-dimensional region the most excitable modes* (m, n) *of a given reaction-diffusion system would depend on the interplay between geometric and chemical aspects. For a given ratio of sides* ($\gamma = L_y/L_x$) *in a rectangular domain, the number of wave peaks in the* x *and* y *directions* (m, n) *changes as the ratio of domain size to range of inhibitor changes, that is, as* E^2 *is altered. Here we have taken* $\gamma = 2$ *by way of example.*

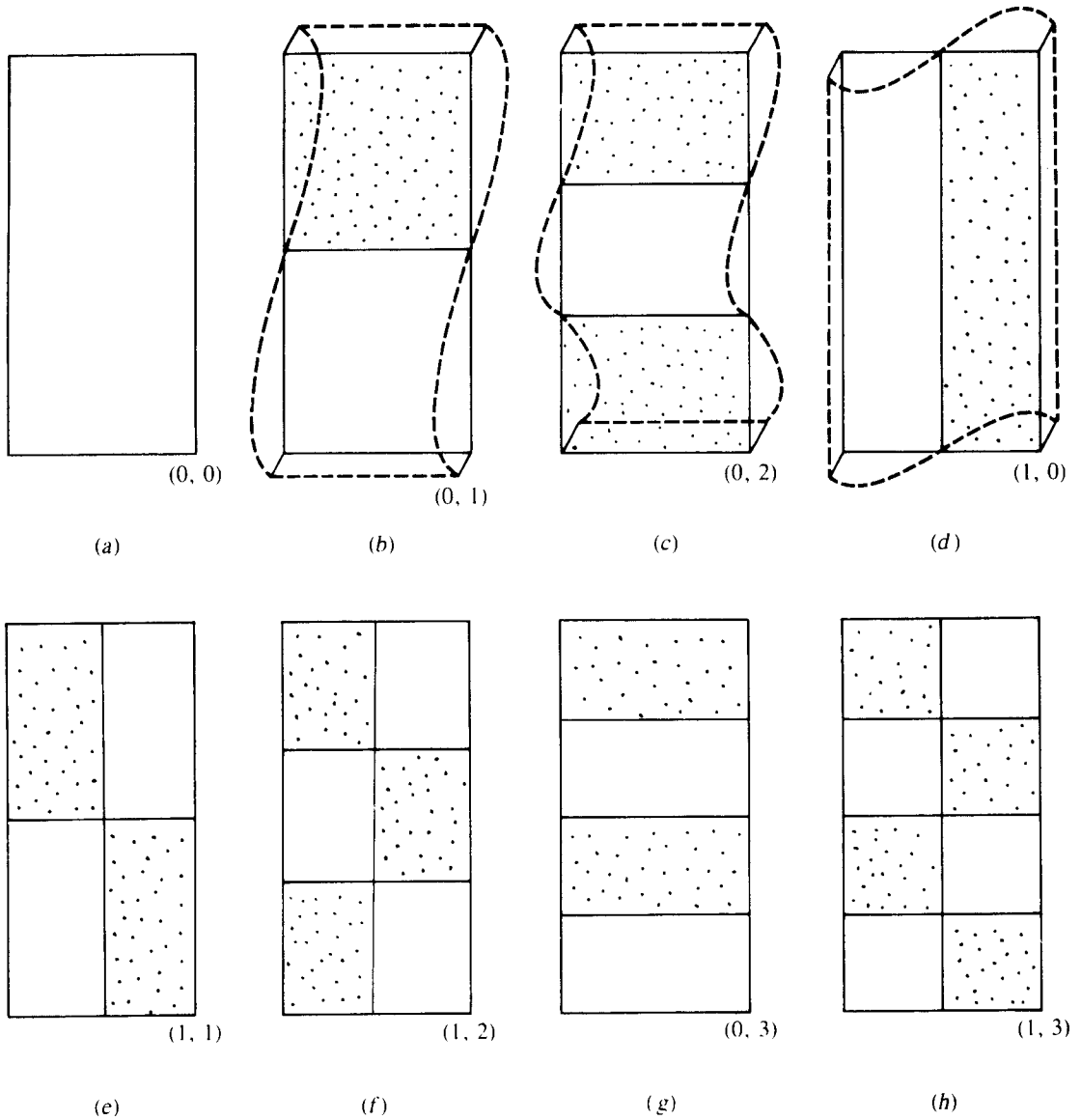

Figure 11.6 *The first several modes* (m, n) *in the sequence predicted in Figure 11.5.* (b ≃ d) *The functional shapes of the excitable perturbations are shown by dotted outlines. Stippled areas are those in which chemical concentrations are higher than their steady-state values. A transition from (a) to (h) (and beyond) would occur if the size of the domain was increased or the size of the chemical range was decreased.*

From such results several observations can be made:

1. The transitions from one mode to the next do not necessarily occur at equal increments of the parameter E^2; some transitions are closer than others.
2. There are certain values of the parameter E^2 that correspond to more than one possible mode. Which mode is actually expressed would then depend on initial

conditions and nonlinear interactions that might tend to stabilize one pattern at the expense of a second.

3. When the domain is wider in one direction (such as in the example in Figure 11.5 $L_y = 2L_x$), there is a tendency for successive subdivisions to occur in the longer direction *before* they occur in the shorter one.

Such results bear several interesting implications in developmental systems. The first of these is that the interactions of diffusing morphogens in a *growing domain* will lead to a discrete succession of patterns. Kauffman et. al. (1978) have proposed an intriguing application of such ideas to the sequence of compartmental subdivision in the imaginal disks of *Drosophila* (see box "Chemical Patterns and Compartments in *Drosophila*"). Murray (1981) has similarly applied these concepts to the spatial succession of patterns that occur on animal coats as the geometry of the domain changes (for example, from an extremity to a broader region such as the body). His model is discussed in greater detail in section 11.8.

Similar ideas with constant domain size and other spatially varying parameters have been used in a number of different contexts. Berding et al. (1983) have shown, for example, that spiral patterns typical of those found on sunflower heads can be generated by a reaction-diffusion system in a circular domain with diffusivities that vary as r^2, where r is the radial distance. Other implications for pattern formation systems are suggested in the problems as topics for independent exploration.

To keep the limitations of this theory in perspective, one must remember that we have been operating under the admittedly artificial assumption that the patterns develop at or close to the critical bifurcation (that is, at the onset of diffusive instability). When a whole *range* of Q^2 values are excitable, one must again address the possible nonlinear effects that lead to considerably more complicated problems.

Although linear analysis of two- or three-dimensional cases is an immediate generalization of the one-dimensional case, there are genuinely novel effects that arise beyond the predictive power of these theories. For large-amplitude perturbations, nonlinear interactions of the waves in the x and y directions play an increasingly important role. The final patterns may be different from those anticipated solely on the basis of the linear approximations.

We summarize some of our findings in the following statements:

1. Pattern formation can only occur if the *range of inhibition* is greater than the *range of activation:*

$$\left|\frac{D_1}{a_{11}}\right| > \left|\frac{D_2}{a_{22}}\right|.$$

2. The type of patterns that then occur depends on two factors:
   - **a.** $\gamma = \dfrac{L_y}{L_x}$ = the geometry of the domain,
   - **b.** $\dfrac{L^2}{D/a}$ = the ratio of the size of the domain to the range of the inhibitor.
3. Parameter variations can lead to changes in the factors described in 2 without affecting the inequality given in 1 or vice versa.

Chemical Patterns and Compartments in Drosophila

Drosophila melanogaster, the common fruitfly, has a number of distinct life stages including egg, larva, pupa, and adult. In the transition from egg to larva, certain groups of cells are reserved in the structures known as *imaginal discs*. Specific parts of these objects will eventually undergo growth and differentiation to produce adult structures. In the larval tissues there are pairs of imaginal discs for eyes, legs, wings, and other body parts. Moreover, each of these may be subdivided into groups of cells destined for specific parts of the final structure. For example, the wing disc has compartments corresponding to subdivisions of a wing including (1) anterior-posterior wing parts, (2) dorsal-ventral wing parts, (3) wing-thorax wing parts, and others.

Based on experimental evidence, it is held that commitment to a given fate is attained as a result of a sequence of stages, each of which increases the restrictions on a given group of cells. It is possible to map cells (according to their positions on the wing disc) with their eventual destinations. (See compartments in Figure 11.7.) Moreover, the sequence of subdivision of the wing discs can also be ascertained (successive boundaries labeled 1 to 5 in the figure). Such compartmentalization appears spontaneously as the imaginal disc grows.

Figure 11.7. *Actual shape and compartmental boundaries of imaginal disc in* Drosophilia. *[From Figure 5 in Kauffman (1977), American Zoologist 17:631–648.]*

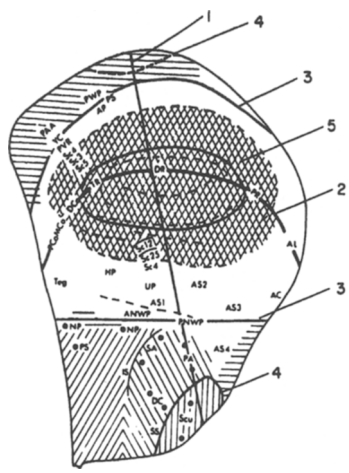

Figure 11.8. *Wave patterns on a disk-shaped domain. The peaks may correspond to places where certain chemical concentrations are high. [From Figure 2 in Kauffman (1977), American Zoologist 17:631–648.]*

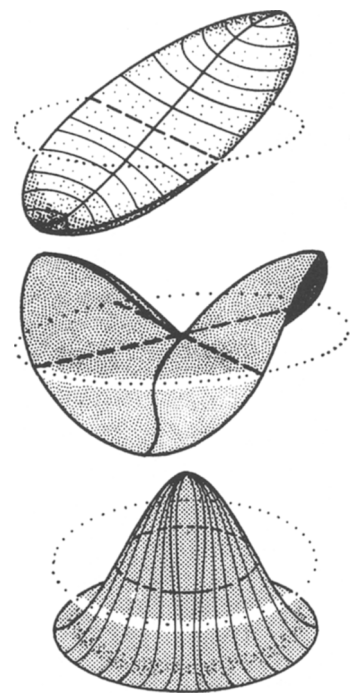

On the basis of such information, Kauffman et. al. (1978) has proposed the following model of successive compartmentalization. Identify the imaginal disc of a wing with an approximate shape of an elliptical region. Consider a hypothetical reaction-diffusion system on this elliptical domain. As the domain grows in size, a discrete sequence of chemical wave patterns is created. Figure 11.8 demonstrates typical wave patterns on circular or elliptical domains. Note a basic similarity to Figure 11.6. The nodal lines of successive patterns that fit on an ellipse as it enlarges are shown in the sequence in Figure 11.9. Projecting all five such predicted boundaries onto a single ellipse results in the compartmentalization shown in Figure 11.10.

This type of sequential process of compartmentalization could, then, arise *spontaneously* by virtue of the fact that an increasing domain size [analogous to increasing L^2 in the expression on the RHS of (56)] causes a succession of modes (m, n) to appear in the chemical patterns that are expressed.

In this example the geometry of the domain is elliptical; however, the basic idea of a succession of patterns (or rather compartmental subdivisions) resulting from a gradual shift in a key parameter (in this case the size) is very much the same as that in a rectangular domain. The actual nodal lines are computed by solving the diffusion equation on a circular disk.

While there is as yet no direct evidence that a reaction-diffusion system underlies the differentiation of *Drosophila* imaginal discs, the time sequence and geometry of compartmentalization proves quite suggestive of some underlying wave phenomenon.

Figure 11.9. *Successive nodal lines on a growing ellipse. [From Figure 3 in Kauffman (1977), American Zoologist 17:631–648.]*

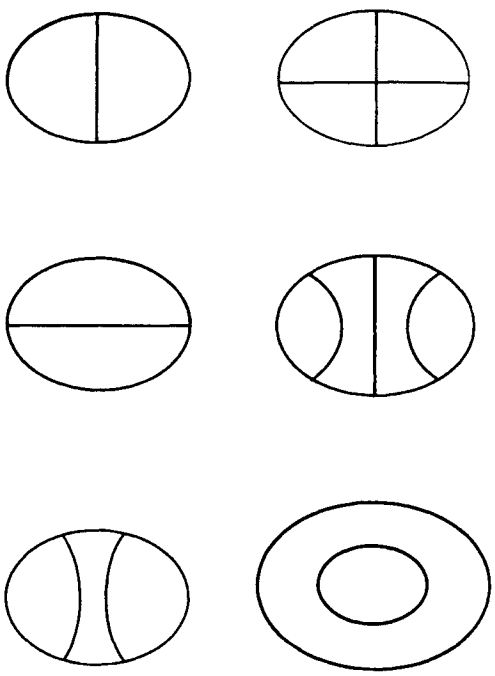

Figure 11.10. *Successive boundaries formed in the idealized elliptical domain. Compare with the actual compartmental boundaries shown in Figure 11.7. [From Figure 6 in Kauffman (1977), American Zoologist 17:631–648.]*

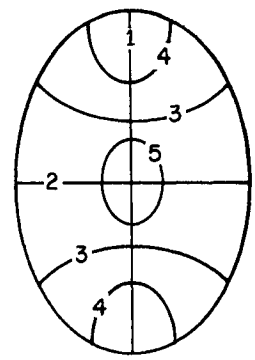

11.8. APPLICATIONS TO MORPHOGENESIS[1]

Since Turing's (1952) paper, two parallel directions have arisen in the research on reaction-diffusion systems. A highly abstract mathematical development characterizes one branch (see, for example, Smoller, 1983 and Rothe, 1984); a more biologically oriented approach characterizes the other. The abstract theories have addressed numerous questions, including the existence of nonstationary (travelling-wave) patterns, spirals, solitary peaks, and fronts. See Fife (1979) for a summary. The more biological directions have formed the connection between specific models and developmental patterns found in biological systems.

The interest of biologists was largely aroused due to contributions by Meinhardt and Gierer in the 1970s. Their work consists predominantly of numerical simulations of reaction-diffusion systems in various geometries. The results often bear a realistic likeness to patterns commonly found in nature. (See the survey in Meinhardt, 1982, and Figures 11.11 to 11.13.)

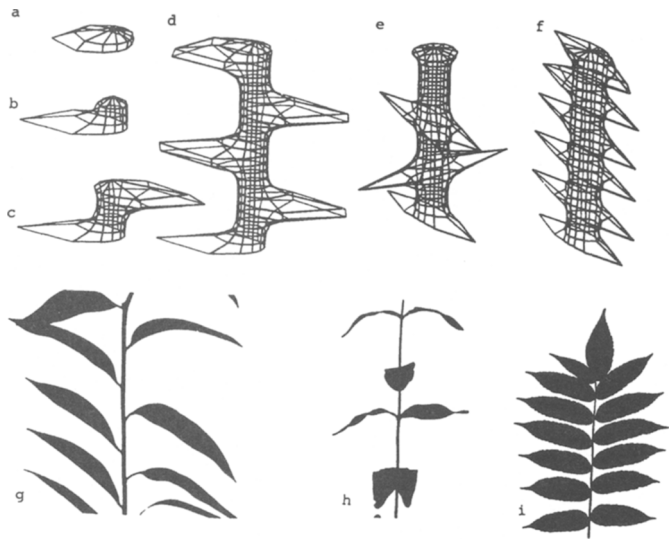

Figure 11.11. *Phyllotaxis, the regular arrangement of leaves on the stem of a plant, was modeled by Meinhardt using an activator-inhibitor mechanism with reaction-diffusion occurring on the surface of the cylindrical stem. (a–f) Locations of activator peaks (obtained by computer simulation); (g–i) Comparable leaf arrangements. [From Meinhardt, H. (1978). Models for the ontogenetic development of higher organisms. Rev. Physiol. Biochem. Pharmacol., 80, 47–104, fig. 5. Reprinted by permission of Springer Verlag.]*

Biology students will find the Meinhardt-Gierer papers readily accessible since very little mathematical analysis is given. Indeed, in the initial stages of their research these authors were unaware of the Turing theory and based their ideas entirely on a familiarity with lateral inhibition in other contexts. They have since de-

1. Part of the material in this section is based on a review by Marjorie Buff.

veloped considerable insight into the combinations of geometry, chemical kinetics, and other effects that lead to interesting patterns. (Not always is their insight imparted to readers.) We now discuss two examples of models proposed by Gierer and Meinhardt.

Consider their first set of equations:

$$\frac{\partial A}{\partial t} = \frac{\rho A^2}{(1 + \kappa A^2)H} - \mu A + D_A \nabla^2 A + \rho_0 \rho, \tag{57a}$$

$$\frac{\partial H}{\partial t} = \rho' A^2 - \nu H + D_H \nabla^2 H + \rho_1. \tag{57b}$$

In these equations A and H are the concentrations of activator and inhibitor respectively. The parameters ρ_0, ρ, μ, ρ', ρ_1, ν, κ, D_A, and D_H reflect source terms, decay rates, reaction rates, and diffusional properties.

One interpretation of terms in equations (57a,b) is as follows. In (57a) the activator A decays spontaneously with rate μ, diffuses at the rate $D_A \nabla^2 A$, and is created in two ways: by a small source term $\rho_0 \rho$, which could vary over space, and by an

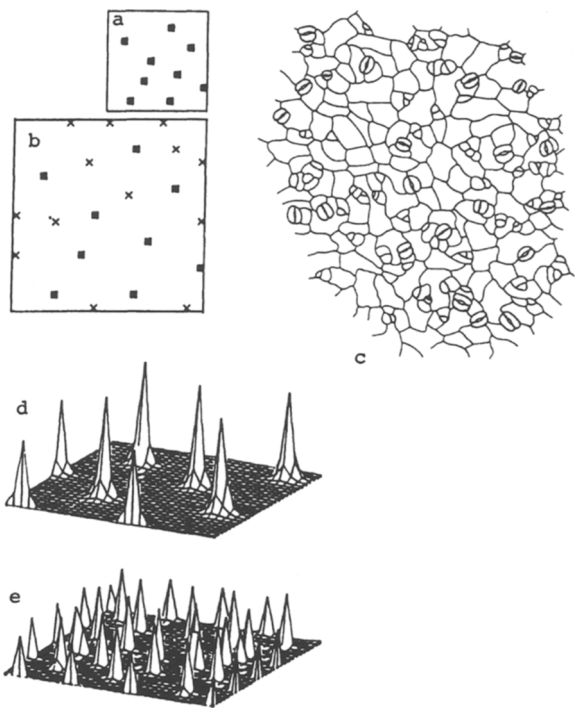

Figure 11.12. *(a,b) Bristlelike patterns and (c) irregularly spaced structures such as* stomata *(pores on leaf surfaces) were also obtained by Meinhardt using activator-inhibitor mechanisms. Results of his simulations are shown in (d) and (e). [From Meinhardt, H. (1978). Models for the ontogenic development of higher organisms. Rev. Physiol. Biochem. Pharmacol., 80, 47–104, fig. 6. Reprinted by permission of Springer Verlag.]*

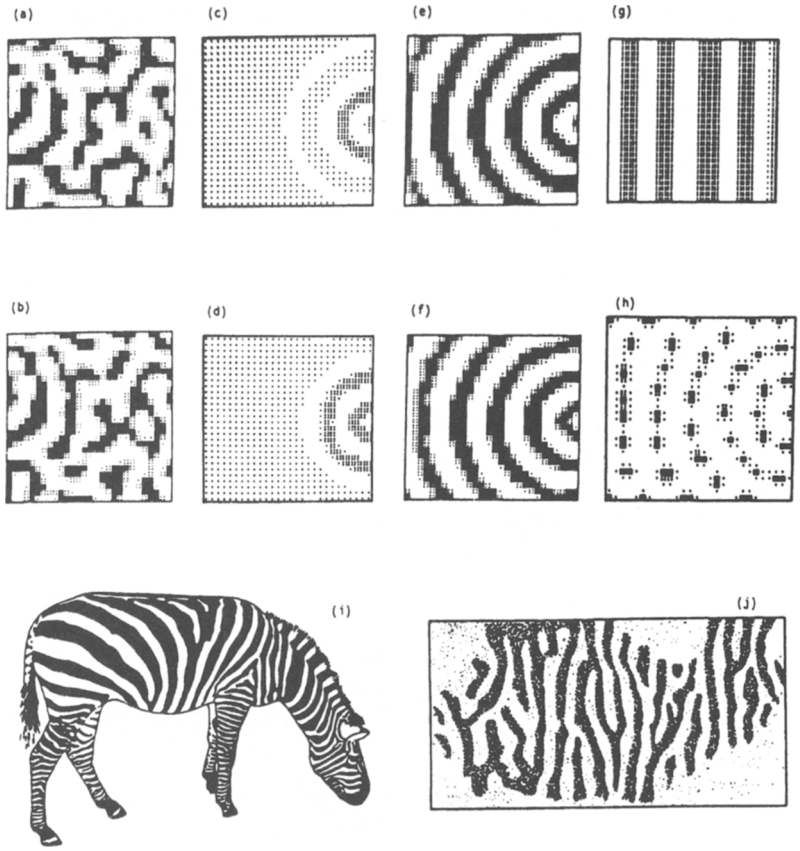

Figure 11.13. *(a–h) stripes and other patterns that can be produced by reaction-diffusion mechanisms in a planar domain (under a variety of initial conditions and chemical interactions). Examples of naturally occurring stripes (i) in zebras and (j) in the visual cortex. [From Meinhardt, H. (1982).* Models of Biological Pattern Formation. *Academic Press, New York, fig. 12.2.]*

autocatalytic reaction represented by the first term of (57a). The sigmoidal kinetic term $A^2/(1 + \kappa A^2)$ depicts a cooperativity effect (an enhanced reaction rate when two molecules of A are present). (See Chapter 7 for the derivation of such terms.) The presence of H in the denominator indicates that the inhibitor would tend to decrease the rate of production of the activator. The effect of these two terms is to limit the maximal activator production rate so that an activator peak will not grow indefinitely.

In equation (57b) the inhibitor H is produced as a result of the cross-catalytic influence of the activator A^2. Hence A indirectly results in its own inhibition. H also decays spontaneously at the rate ν, diffuses ($D_H \nabla^2 H$), and has a small activator-independent source term ($\rho' A^2$) that prevents pattern formation at low concentrations of the activator. To produce patterns with particular polarity, Gierer and Meinhardt

have often biased the source distribution by assuming a convenient spatial dependence. There has been some controversy regarding the validity of this approach.

A second simpler set of equations they have used is given in the box and analyzed as an example illustrating the techniques developed in this chapter. (An interpretation is left as a problem for the reader.)

Example

Gierer and Meinhardt applied the following set of equations to a pattern-forming process.[2] Define

$a(x, y; t)$ = concentration of activator at location (x, y) and time t,
$h(x, y; t)$ = concentration of inhibitor at location (x, y) and time t.

Then

$$\frac{\partial a}{\partial t} = \frac{c_1 a^2}{h} - a\mu + D_a \nabla^2 a, \tag{58a}$$

$$\frac{\partial h}{\partial t} = c_2 a^2 - \nu h + D_h \nabla^2 h. \tag{58b}$$

A homogeneous steady state $(\bar{a}, \bar{h})$ *satisfies*

$$\left.\begin{aligned} \frac{c_1 \bar{a}^2}{\bar{h}} - \bar{a}\mu = 0 \\ c_2 \bar{a}^2 - \nu \bar{h} = 0 \end{aligned}\right\} \Rightarrow \begin{aligned} \bar{a} &= \frac{c_1 \nu}{c_2 \mu}, && (59a) \\ \bar{h} &= \frac{c_1^2 \nu}{c_2 \mu^2}. && (59b) \end{aligned}$$

The Jacobian for this system is

$$\mathbf{J} = \begin{pmatrix} \dfrac{2c_1 a}{h} - \mu & \dfrac{-c_1 a^2}{h^2} \\ 2c_2 a & -\nu \end{pmatrix}_{ss} = \begin{pmatrix} \mu & \dfrac{-\mu^2}{c_1} \\ \dfrac{2c_1 \nu}{\mu} & -\nu \end{pmatrix}, \tag{60}$$

so

$$\det \mathbf{J} = \mu\nu(-1 + 2) = \mu\nu. \tag{61}$$

The condition for diffusive instability is

$$\mu D_a - \nu D_h > 2(\mu\nu)^{1/2}(D_a D_h)^{1/2}, \tag{62a}$$

2. In the original paper $c_1 = c_2 = c_j$; this leads to inconsistency in the dimensions and so has been modified here.

or

$$\epsilon\delta - \frac{1}{\epsilon\delta} > 2, \tag{62b}$$

where

$$\epsilon = \left(\frac{\mu}{\nu}\right)^{1/2}, \qquad \delta = \left(\frac{D_h}{D_a}\right)^{1/2}. \tag{62c}$$

Problem 17 shows that (62b) implies that $\epsilon\delta$, which must be a positive quantity, satisfies

$$\epsilon\delta > 1 + \sqrt{2}. \tag{63}$$

At the onset of instability, the most excitable modes are characterized by

$$Q^2 = q_x^2 + q_y^2 = \frac{1}{2}\left(\frac{\mu}{D_a} - \frac{\nu}{D_h}\right). \tag{64}$$

Note that the instability condition depends only on dimensionless ratios such as ϵ and δ, whereas Q^2 carries dimensions of $(1/\text{distance})^2$ and thus depends on absolute magnitudes of the diffusion coefficients.

Figures 11.11 through 11.13 are a sample of some of the elegant patterns produced over the years by Meinhardt and Gierer. Unfortunately, rarely do they specify the exact conditions and parameter values used in their simulations. It has been shown (see Murray, 1982) that the sets of parameter values leading to pattern formation in these models are unrealistically restrictive.

Bridging the gap between the totally abstract and the predominantly biological literature are several partly theoretical papers whose main concern is *explaining* properties of patterns on the basis of chemical interactions and geometric considerations. Among these are several classic contributions by Murray, including his model for animal coat patterns briefly highlighted here.

Murray (1981*a*,*b*) describes a hypothetical mechanism for *melanogenesis* (synthesis and deposition of *melanin* granules, which are responsible for the dark pigmentation of mammalian skin and fur). It is assumed that reactions and diffusion occur on the plane of an active membrane and that the kinetics stem from a substrate-inhibited enzymatic reaction between two substances, S and A whose concentrations we represent by s and a (see problem 21).

In dimensionless form the model equations are as follows:

$$\frac{\partial s}{\partial t} = \gamma g(s, a) + \nabla^2 s, \tag{65a}$$

$$\frac{\partial a}{\partial t} = \gamma f(s, a) + \beta\nabla^2 a, \tag{65b}$$

where

$\beta = D_a/D_s$ = ratio of diffusion coefficients,

γ = dimensionless parameter proportional to the area of the domain,

g, f = the functions given in Figure 8.14.

These phase-plane drawings reveal a cubic nullcline configuration, with an intersection that depends on the size of a parameter K, which represents the degree of substrate inhibition. Decreasing K results in the transition of (a) to (b) to (c) in Figure 8.14. While these equations do not permit easy analysis since their steady state cannot be explicitly obtained, it transpires that only in one configuration, namely the one shown in Figure 8.14(b), is diffusive instability possible. (See problem 21.) This leads to a suggestive but entirely hypothetical mechanism for the development of the patterns.

Suppose that there is a substance that inhibits melanogenesis whose concentration early in embryonic development is high. Suppose that, at later stages, a decrease in the level of this inhibitor is brought about. At that point, diffusive instability leading to spatial patterns will occur, resulting in the prepattern for coat markings. If, however, there is further decrease in inhibition, diffusive instability will no longer be possible, and no further development of pattern can take place.

A second prediction concerns the interchange between size or geometry and the nature of the patterns. Variations in the area of the domain can be conveniently depicted by variation in the parameter γ (see Figure 11.14). Murray demonstrates that as γ increases, there is a succesion of excitable modes, as we discovered in Section 11.7. If one of the dimensions (for example, L_x, length in x direction) is sufficiently small compared to the other (L_y), there is a tendency for a succession of patterns with modes characterized by $m = 0$ and $n = 1, 2, \ldots, k$ *before* the first pattern with $m \geq 1$ is obtained. This means that stripes predominate on this narrow domain and spots are more characteristic of wider regions. (See Figure 11.6(g) for "stripes" and Figure 11.6(f) for "spots".) A common feature in many spotted animals is that their slender extremities retain a striped pattern, as predicted by this theory.

As an endpoint of his model Murray terminates with a whimsical but ingenious prediction about pigmentation patterns on tails. Tails are often broader at their base than at their end, so that their shape is roughly conical. If the fur is removed and the cone opened by a longitudinal bisection, one obtains a triangular domain with a narrow end and a broader base of radius r_0. This geometry can be represented by letting the size parameter γ vary gradually across the length of the domain (see Figure 11.15). According to our previous discussion, such variation is consistent with a transition from stripes at the thin one-dimensional end to spots at the broader base. The opposite transition would be inconsistent and thus contradictory of the theory. To date, animals with the proper tail patterns have been found in great abundance. As yet no single possessor of an inconsistent tail has reportedly been sighted. (See Figure 11.16.)

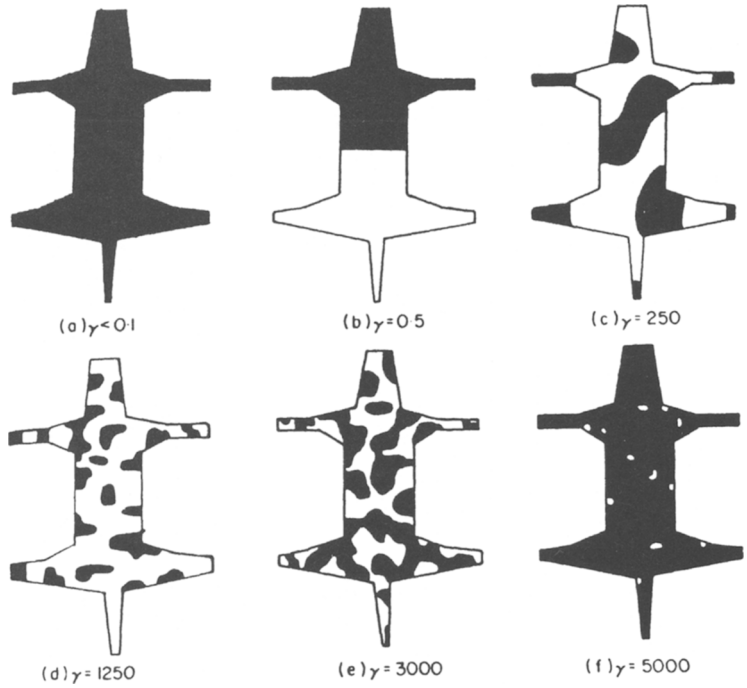

Figure 11.14. *Effects of size of an animal on the patterns formed on its coat by a reaction-diffusion prepattern mechanism proposed by Murray (1981). As the size parameter γ changes from (a) to (f), a succession of patterns (typical of different animals) occurs. For very large domains the nonlinear effects make a substantial contribution, so that patterns are no longer predictable based on linear theory. [From Murray, J. D. (1981). A prepattern formation mechanism for animal coat markings.* J. Theor. Biol. 88, *161–199, fig. 8. Reprinted by permission of Academic Press.]*

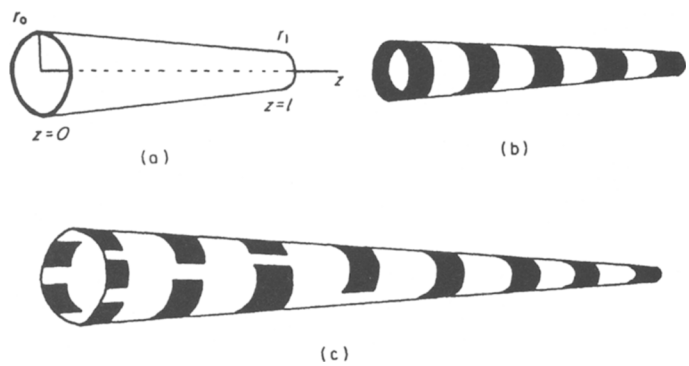

Figure 11.15. *Effects of geometry on patterns. Reaction diffusion on a conical surface (such as a tail) may result in a progression from stripes to spots in only one way. The spots tend to appear if (a) r_0, the radius of the base, is large enough to admit several chemical "peaks" around its circumference, as in (c) [From Murray, J. D. (1981a). A prepattern formation mechanism for animal coat markings.* J. Theor. Biol., 88, *161–199, fig. 5. Reprinted by permission of Academic Press.]*

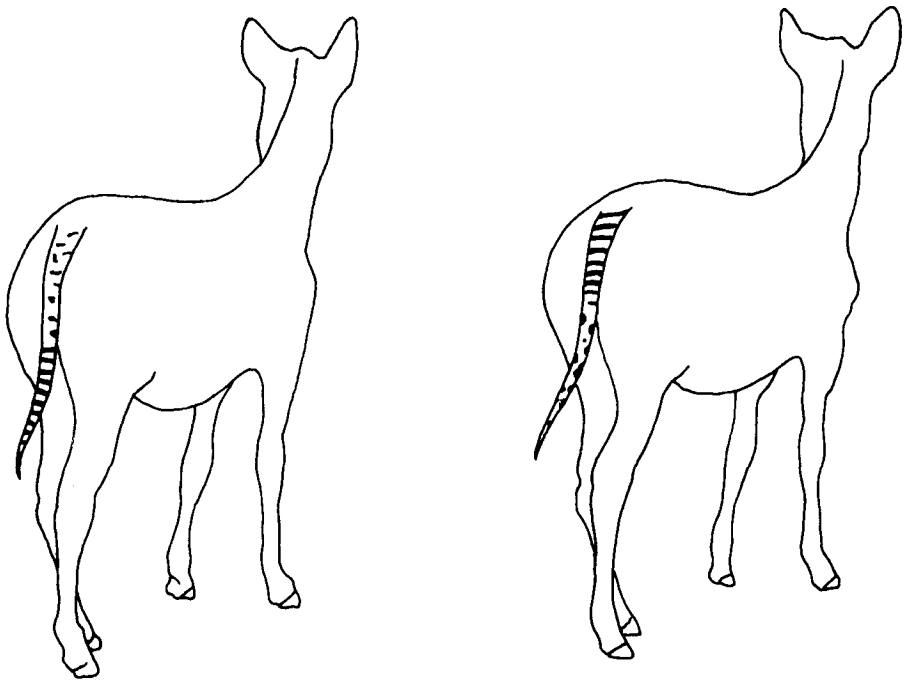

(*a*) (*b*)

Figure 11.16. *(a) Tail pattern predicted by linear theory; (b) tail pattern impossible by linear theory.* *[Drawn by Marjorie Buff.]*

11.9. FOR FURTHER STUDY

Patterns in Ecology

A recurring theme in this book is that mathematical models lead us to draw parallels between situations that may seem totally unrelated on first inspection. Analogies between the microscopic molecular realm and the macroscopic population level have appeared repeatedly in previous discussions. For this reason it is to be anticipated that spatial patterns emerging from unstable uniform distributions may occur in ecological settings as well, particularly in species that interact and disperse at different rates.

The first prediction that this may indeed occur appears in Segel and Jackson (1972). The authors realized that a similarity between activator-inhibitor chemicals and prey-predator species exists. However, merely "tinkering" with the Lotka-Volterra models, augmented by dispersal terms, was unsuccessful in producing diffusive instability. One of the attractive features of the Segel-Jackson paper is the detailed discussion of the motivation that led to their specific model. (Rarely are authors as candid about the development of a theory.) A good topic for advanced

students would be to independently address the following question posed by the authors:

> [What are] the characteristics of a situation where uneven geographic distribution of predator and prey would be mutually advantageous? (1972, p. 553.)

As a second stage, students might attempt to write their own model and test the Turing criteria (32a,b) and (38) before turning to the papers provided in the references by way of a comparison. For reasons outlined in their paper, Segel and Jackson (1972) considered the following set of equations:

$$\text{Prey:} \qquad \frac{\partial V}{\partial t} = VR(V) - AVE + \mu_1 \nabla^2 V, \tag{66a}$$

$$\text{Predators:} \qquad \frac{\partial E}{\partial t} = BVE - ME - CE^2 + \mu_2 \nabla^2 E, \tag{66b}$$

where $V(x, t)$ = the prey ("victims"), $E(x, t)$ = the predators ("exploiters"), and

$$R(V) = K_0 + K_1 V. \tag{67}$$

Interpretation of the model and its parameters is left as an exercise.

Patchy distributions of populations have been observed in nature under numerous conditions. One well-documented example is *plankton,* the microscopic aquatic organisms often found in uneven distributions at or close to the surface of the water. (See Okubo, 1980, for review and references.) Plankton actually consists of a multitude of uni- and multicellular organisms, which are frequently characterized simply as *zooplankton* or *phytoplankton.* The latter are capable of photosynthesis; like higher plants they are in a sense self-sufficient, relying mainly on sunlight for their energy. The former are predatory, feeding on phytoplankton and on each other.

Patchy distributions of plankton may arise from different mechanisms, and a conclusive explanation has not been given. However, the idea that the natural dispersal rate of these microscopic organisms might lead to instability of the type described in this chapter is rather intriguing.

Mimura and Murray (1978) discuss a slightly different theoretical model given by the equations

$$\frac{\partial P}{\partial t} = [f(P) - Q]P + \mathcal{D}_P \frac{\partial^2 P}{\partial x^2}, \tag{68a}$$

$$\frac{\partial Q}{\partial t} = -[g(Q) - P]Q + \mathcal{D}_Q \frac{\partial^2 Q}{\partial x^2}, \tag{68b}$$

where P is phytoplankton and Q is zooplankton. A particular assumption made is that the graph of $f(P)$ has a "hump" and that $g(Q)$ has a positive slope (see Figure 11.17). A typical set of functions proposed in the paper is the following:

$$f(P) = K(K_0 + K_1 P - P^2), \tag{69a}$$

$$g(Q) = K_2 + K_3 Q. \tag{69b}$$

Noting that $f(P)$ represents the prey growth rate, one might attribute its hump

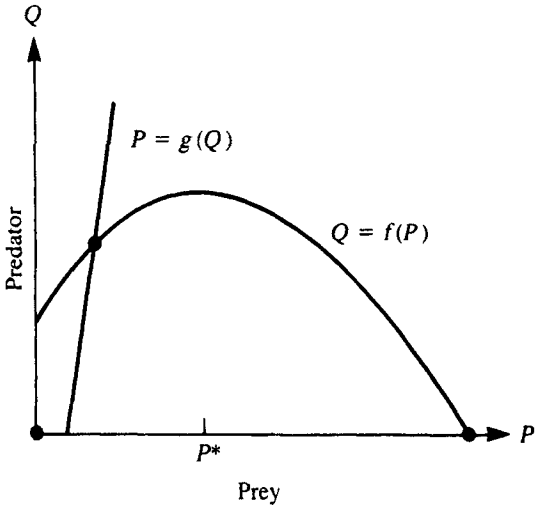

Figure 11.17. *The predator-prey phase plane for equations (68a,b) with* f(P) *and* g(Q) *given by equations (69a,b) in a model by Mimura and Murray (1978). Note the hump effect in* f(P).

to an Allee effect (see Section 6.1). The authors prove that the hump in f leads to a property crucial for realistic solutions; namely, that spatial patterns resulting from diffusive instability will in certain limiting cases tend to have alternately low and high *plateaus* of population density. Models in which the hump effect is absent tend to have sharply peaked spikelike patterns of prey density. These are considered to be less realistic. (Proof rests on singular perturbation analysis and may be too advanced for some readers.)

Evidence for Chemical Morphogens in Developmental Systems

How has the chemical theory for morphogenesis fared in light of empirical research? The true test of such theories would be to isolate and characterize chemical substances that have demonstrable morphogenetic effects. This is a challenging task given that such substances, if they are present, may be found in minute quantities.

Work in this direction is being carried out. It is said that in an attempt to isolate such substances in one accessible system, the *hydra*, it was necessary to process and analyze material from several tons of sea anemone, which are relatives of this organism. (H. C. Schaller 1973, 1976).

The hydra is a small freshwater organism (3 to 4 mm long) with the ability to regenerate body parts [see Figure 11.18(*a*)]. Any small piece excised from its body column (a roughly cylindrical shape) can form a whole new hydra by making a tentacled "head" and a "foot" in the appropriate ends. Chemical studies by Schaller and others have revealed several molecular morphogenetic substances, among them the *head activator* and the *head inhibitor*. Characterization of the nature and interactions of such substances is proceeding, but many details are still missing.

Based on this partial characterization, Kemmner (1984) has formulated a model for a possible reaction-diffusion system in the hydra [see Figure 11.18(*b*) and Table 11.1]. The evidence indicates a somewhat more subtle underlying mechanism,

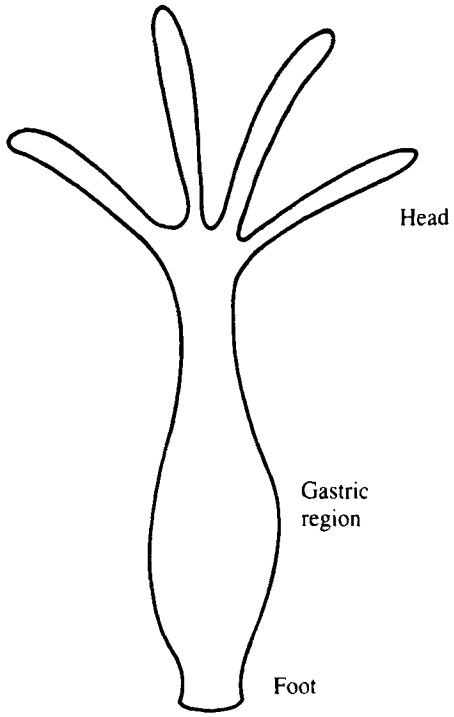

(*a*)

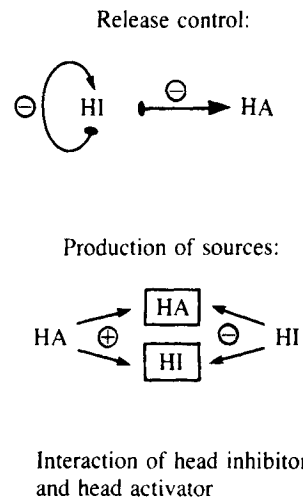

(*b*)

Figure 11.18. *(a) Simple diagram of the hydra, a freshwater polyp. (b) Chemicals identified as morphogenetic substances in hydra. The head inhibitor (HI) inhibits both its own release and the release of head activator (HA) from sources. The formation of sources depends on the presence of HA. In this sense HA is autocatalytic. [(b) From Kemmner, W. (1984). Head regeneration in* Hydra*: Biological studies and a model. In W. Jager and J. D. Murray, eds.,* Modelling of Patterns in Space and Time*. Springer-Verlag, New York, fig. 3.]*

Table 11.1 ***Properties of morphogenetic substances from hydra controlling head and foot formation.***

Morphogen	*Molecular Weight*	*Nature*	*Purification (x-fold)*	*Active Concentration*	*Gradient*
Head activator	1142	Peptide	10^9	10^{-13} M	
Head inhibitor	<500	Nonpeptide	10^5	$<10^{-9}$ M	
Foot activator	~1000	Peptide	10^5	$<10^{-9}$ M	
Foot inhibitor	<500	Nonpeptide	10^4	$<10^{-3}$ M	

Source: Kemmner, W. (1984). Head regeneration in *Hydra:* Biological studies and a model. In W. Jager and J. D. Murray, eds., *Modelling of Patterns in Space and Time*. Springer-Verlag, New York, table 1.

namely that one of the two substances inhibits the release of both from preexisting sources. Moreover, self-enhancement arises not by direct autocatalysis but rather by virtue of the fact that sources of the substances are restored (if removed) by the presence of the activator. The paper by Kemmner and other references provided therein are recommended as good sources for further independent investigation.

Few other systems have so readily revealed their secrets to us. It would at present appear that many developmental systems are not governed (even partially) by simple pairs of chemical species. The Turing theory as yet remains a vivid paradigm rather than an accurate description of any one real morphogenetic event.

A Broader View of Pattern Formation in Biology

A recent review paper by Levin and Segel (1985) provides a general survey and further recent references on pattern-generating processes. While the Turing theory still ranks among the top contenders for pattern-forming mechanisms, a variety of different theories have been formulated for special systems. It has been shown in recent papers that neural networks (with excitatory and inhibitory elements) can generate patterns of various sorts. A number of self-organizing systems such as cellular automata and clonal organisms (both described in boxes to come), which are governed by simple recursive rules, have been studied. Mechanochemical theories have addressed the morphogenesis of tissues formed by migration and movement or deformation of cells. Some of these theories are entirely unrelated to those described in this chapter. Others do share certain common conceptual features; for instance, many are based on the property of lateral inhibition. One example, to be described here, is drawn from neural interactions.

As previously mentioned, nerves communicate with one another over great distances. One can define the *range of activation* and the *range of inhibition* in a neural network as the average distance over which one neuron transmits stimulatory or inhibitory signals to its neighbors via synapses. The effect modulated by a synapse can be either positive (excitatory) or negative (inhibitory) to the neuron on which it impinges. Thus, interactions over a distance in a neural network are *analogous* to interactions over the diffusional range of activator-inhibitor chemicals in the Turing system we described. The details of the mechanism and its mathematical description, though, are different.

The boxes in this section give a brief survey of recent work in other theories of pattern formation. For details and further sources, consult the appropriate References.

Patterns in neural networks: **Visual Hallucinations**

The patterns shown in Figure 11.19 are experienced during drug-induced visual hallucinations. In the figure, designs on the left-hand side are visual images that are perceived to be centered at the *fovea* (the center of the visual field in the *retina* of the eye). The

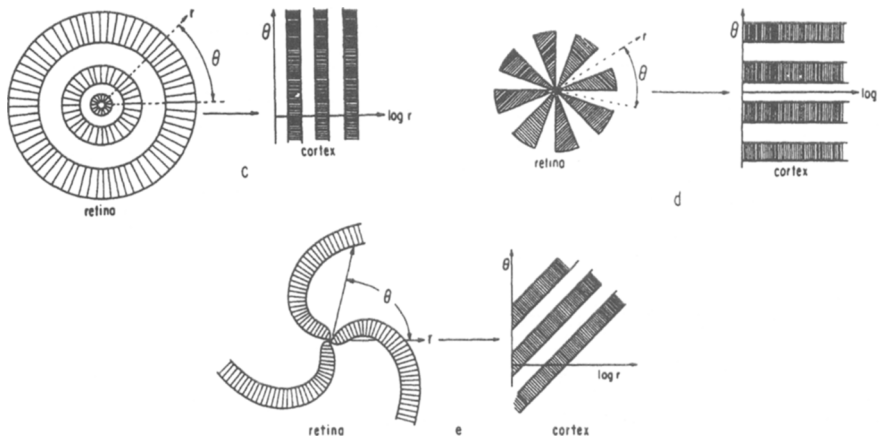

Figure 11.19. *Visual hallucination patterns in retinal and cortical coordinates: On the RHS are patterns that arise in some possibly small region of the visual cortex as a result of long-range inhibition and short-ranged activation within the cortical neural network. On the LHS are the actual hallucination patterns perceived as though they are on the retina. (A log-polar to rectangular coordinate transformation governs the correspondence between the patterns on the LHS and those on the RHS.) [From Ermentrout, G. B., and Cowan, J. (1979). Mathematical theory of visual hallucination patterns.* Biol. Cybernet., 34, *137–150, fig. 2.]*

corresponding designs on the right-hand side are patterns of neural excitation on the *visual cortex* (an area of the brain that processes visual signals). The correspondence, called the *retinocortical map*, has been established empirically according to Ermentrout and Cowan (1979). It is essentially a coordinate transformation from polar coordinates in the retina to cortical rectangular coordinates in the cortex.

It is believed that hallucination patterns form in the cortex, which is a complex neural network, even though no visual stimuli are present on the retina. Ermentrout and Cowan (1979) proposed the theory that patterns of excitation in the cortex arise spontaneously as a result of instability of a uniform resting state. They further suggest that instability occurs when enhanced excitatory and decreased inhibitory effects of neural synapses occurs, for example, as a result of chemical changes in the brain. In their 1979 paper they demonstrate that spatial patterns such as those on the right side of Figure 11.19 are possible in neural networks with the property of lateral inhibition. An informal presentation of these results is to be found in Ermentrout (1984).

For other neural network patterns, see Swindale (1980) and Ermentrout et al. (1986).

A Spatially Discrete Lateral-Inhibition Model

In a discrete model for vertebrate skin patterns proposed by Young (1984), a differentiated cell located at $R = 0$ exerts an effect on its neighbors according to the activation-inhibition field shown in Figure 11.20. w_1 and w_2 are respectively the net positive and negative effects; R is radial distance; and R_1 and R_2 are analogous to the ranges of activation and inhibition respectively. If the net effect on some undifferentiated cell (summed up over contributions of all its neighbors) is positive, the cell will differentiate into a pigmented cell. Patterns thus produced by computer simulations for $R_1 = 2.3$, $R_2 = 6.01$, $w_1 = 1$, and four values of w_2 are shown. Note that, although diffusion is not explicitly depicted, the mechanism for pattern formation is that of lateral inhibition: local activation and long-range inhibition.

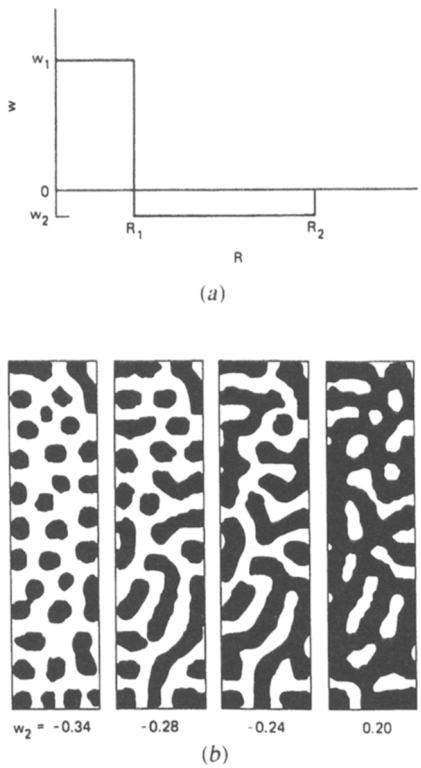

Figure 11.20. *(a) A discrete activation-inhibition field. (b) Patterns produced from an initially random distribution of differentiated "cells" (not shown) by successive iterations using the spatial effects given in (a). [Reprinted by permission of the publisher from "A local activator-inhibitor model of vertebrate skin patterns" by D. A. Young,* Math. Biosci., 72, *figs. 1b and 2, pp. 51–58. Copyright 1984 by Elsevier Science Publishing Co., Inc.]*

Mechanochemical Patterns

In many developing systems, groups of cells are seen to migrate or move collectively in forming the final shape of some part of an organism. The elasticity, adhesiveness, and relative affinities of different cells for one another then governs the succession of shapes or patterns that result in these systems. Models based on underlying physical, mechanical, and chemical processes have been explored recently by Murray and Oster (1984) and Odell et al. (1981).

Odell et al. (1981) explored the process of *gastrulation*, part of the early development of an embryo. They modeled each cell as an element that could stretch and distend in shape, subject to properties of its internal structural components. In the computer simulations (shown in Figure 11.21) the group of cells is seen to undergo a sequence of shapes eventually forming the *gastrula* in which an invagination is present. (These simulations depict a two-dimensional analog of a three-dimensional shape.)

For other references, see Oster et al. (1983), Murray and Oster (1984), also Sulsky et al. (1984).

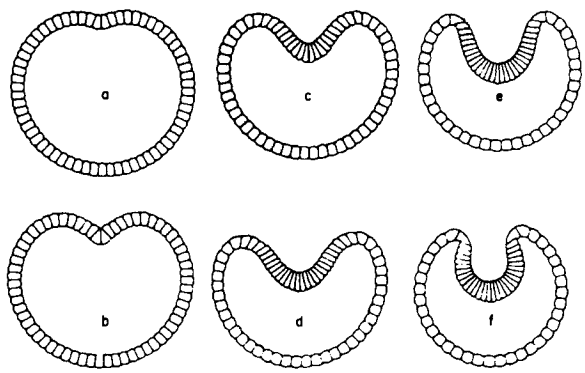

Figure 11.21 *(a–f) Computer simulation of gastrulation in the sea urchin. [From Odell, G. M., Oster, G., Alberch, P. and Burnside, B. (1981). The mechanical basis of morphogenesis. Develop. Biol., 85, 446–462, fig. 7.] Academic Press, New York.*

Patterns in Cellular Automata

One class of models for self-organizing systems is the *cellular automata*. These theoretical systems consist of a discrete number of "cells" (arranged, for example, in a row). Each cell has some initial *state* (represented by an integer). The automaton is governed by a *transition rule*, which assigns a new state to every cell based on the current state of the cell and of its neighbors. The mathematical properties of cellular automata have been described in numerous papers by S. Wolfram (1984a,b). Such systems are more popularly known for their striking patterns, which are readily studied by simple computer simulations (see Figure 11.22). See Wolfram (1984*a*) for a general review and biological applications.

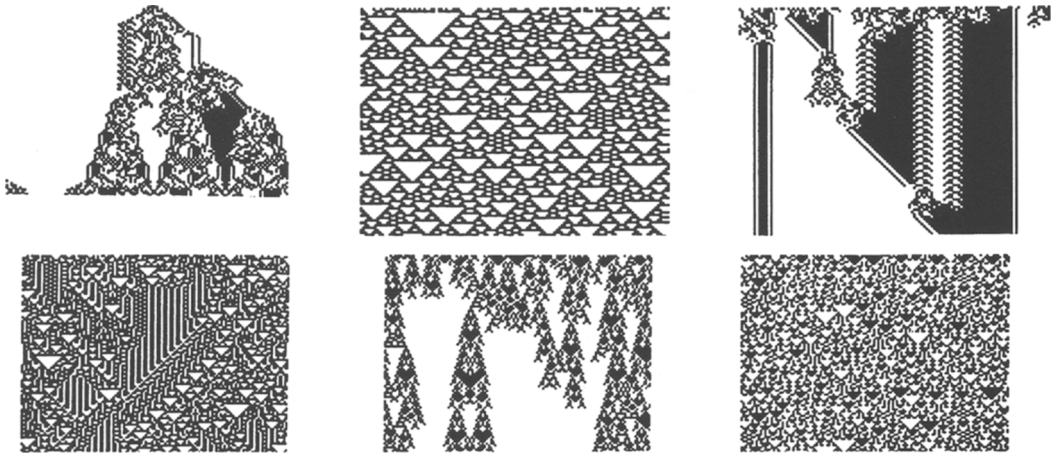

Figure 11.22. *In these one-dimensional cellular automata, the initial state of a row of cells (at the top of each frame) changes successively as the transition rule is applied. The resulting space-time patterns are created. [From Figures selected from Wolfram, S. (1984). Universality and complexity in cellular automata,* Physica, 10D. *Reprinted by permission of North-Holland Physics Publishing.]*

Patterns in clonal organisms

Many simple organisms grow by adding new segments to preexisting structures (see Sections 1.9 and 10.4). Branching of filaments is one instance of clonal growth. The patterns shown in Figure 11.23 are produced by a simple set of recursive rules applied successively in a numerical simulation of the growth of such networks. Here the final patterns result from local interactions of parts of the structure and the continual random formation of new segments by branching. For other references on a similar subject see Cohen (1967) and Jackson et al. (1986).

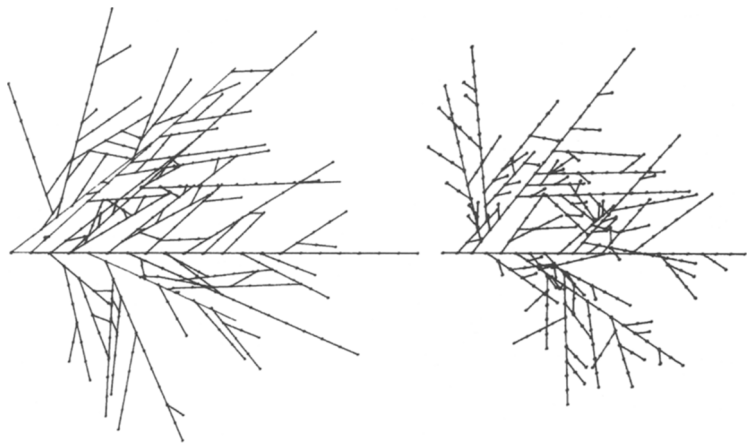

(*a*) (*b*)

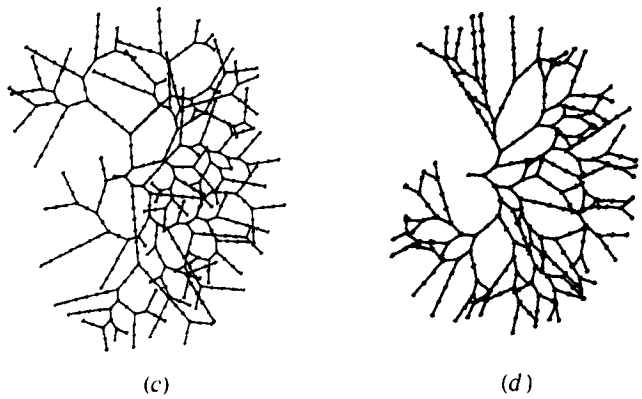

(c) (d)

Figure 11.23. *Patterns formed by computer simulations of simple branching rules. (a,b) Branching occurs only along a preexisting branch. (c,d) Branching is* apical. Anastomoses *(reconnections) occur between apices and branches in (a,d) and between apices only in (b,c). [Simulation program written and figures produced by Richard Fogel.]*

PROBLEMS*

1. *Cellular aggregation*

(a) Justify each of the terms appearing in equations (2a,b).

(b) Verify that equations (6a,b) and (7a,b) are obtained by expanding (2a,b) and then linearizing about the steady state $(\bar{a}, \bar{c})$.

***(c)** In order for linearization to be a valid approximation it is necessary to assume that the perturbations a' and c' are small. What else must be assumed about the perturbations so that nonlinear terms in (7a,b) can be neglected? How does this assumption influence the validity of the special forms (9a,b)?

(d) Verify that equations (14a–c) are obtained from (13).

(e) Explain the reasoning used to deduce condition (16) from equations (14a–c).

(f) Show that if equations (2a,b) for $a(x, t)$ and $c(x, t)$ have the no-flux boundary conditions of equations (17a,b) imposed on them, then the perturbations $a'(x, t)$ and $c'(x, t)$ must also satisfy the same no-flux boundary conditions.

*Problems preceded by an asterisk (*) are especially challenging.

(g) The functions $\sin x$ and $\cos x$ have periods of 2π. Why then are permissible values of the wavenumber q given by equation (18) rather than by $q = n(2\pi)/L\,(n = 0, 1, 2, \ldots)$?

2. Which of the following procedures would tend to promote the onset of aggregation?

(a) Placing barriers so that the domain is subdivided into several subregions.

(b) Increasing the ambient cAMP concentration in the initial homogeneous state.

(c) Causing the amoeba to reproduce vigorously before entering the starved state.

(d) Raising the temperature.

(e) Adding *phosphodiesterase* to the medium.

3. For $n = 1$, inequality (19) can also be written in the form

$$\frac{1}{f}\frac{(L/\pi)^2}{\chi\bar{a}} < \frac{1}{k + (\pi/L)^2 D}\frac{(L/\pi)^2}{\mu}.$$

(See Segel, 1980.)

(a) Verify this fact.

(b) Interpret the meaning of each of the four terms in the equation.

(c) Give a verbal interpretation of the above aggregation condition.

4. What quantity in the model discussed in Section 11.3 depicts the size of the aggregation domain? (Observe that the amoeba density does not enter into this quantity.)

5. *Possible modification of the cellular aggregation model*

(a) Suggest how such quantities as χ, μ, f, and k (assumed constant in the simplest model) might depend on the variables a and c.

(b) How would equations (2a,b) and (6a,b) change under the assumption that the parameters in (a) are nonconstant? [You may wish to take general forms such as $\chi = \chi(c)$, $k = k(a)$, $f = f(c)$, and so forth.

(c) How would equations (8a,b) change?

***(d)** By assuming small perturbations of the form shown in (9a,b) and proceeding with a similar analysis, derive a stability condition analogous to (16).

***(e)** Use your result to argue what properties of the functions χ, μ, f, and k might promote aggregation.

6. Generalize the Keller-Segel model to rectangular two-dimensional aggregation domain of dimensions $L_x \times L_y$.

7. Lauffenburger and Kennedy (1983) suggest a model for the chemotaxis of phagocytes (white blood cells) towards high bacterial densities (part of the tissue inflammatory response to bacterial infection). A set of dimensionless equations that they studied are:

$$\frac{\partial v}{\partial t} = \rho \frac{\partial^2 v}{\partial x^2} + \frac{\gamma v}{1 + v} - \frac{uv}{\kappa + v}$$

$$\frac{\partial u}{\partial t} = \frac{\partial^2 u}{\partial x^2} - \delta \frac{\partial}{\partial x}\left(u \frac{\partial v}{\partial x}\right) + \alpha(1 + \sigma v - u)$$

where

v = dimensionless bacterial density,

u = dimensionless phagocyte density.

γ = ratio of maximum bacterial growth rate to maximum phagocyte killing rate;

σ = ratio of enhanced phagocyte emigration rate to normal "background" emigration rate;

κ = ratio of inhibition effect of increasing bacteria density on bacterial growth to inhibition effect of killing;

α = ratio of phagocyte death rate to maximum phagocytic killing rate.

(See problem 11 of Chapter 10.)

(a) Show that the stability of a uniform steady state to uniform (i.e. space-independent) perturbations is governed by the Jacobian matrix

$$\mathbf{J}_l = \begin{bmatrix} \dfrac{\gamma}{(1 + v)^2} - \dfrac{\kappa u}{(\kappa + v)^2} & -\dfrac{v}{\kappa + v} \\ \alpha\sigma & -\alpha \end{bmatrix}.$$

(b) What would be the corresponding matrix $\mathbf{J}$ governing stability of nonuniform perturbations?

(c) For the steady state $(\bar{u}, \bar{v}) = (1, 0)$ show that the eigenvalues of the matrix in part (b) are

$$\lambda_1 = -\rho q^2 + \gamma - \frac{1}{\kappa}, \qquad \lambda_2 = -q^2 - \alpha.$$

(d) Which mode (i.e. which value of q) is the most likely to cause instability? What is the implication?

(e) For the second steady state of the equations, $\bar{v} > 0$, $\bar{u} = 1 + \sigma\bar{v}$, show that the stability matrix is

$$\mathbf{J} = \begin{bmatrix} -\rho q^2 + F(\bar{v}) & -H(\bar{v}) \\ \delta\bar{u}q^2 + \alpha\sigma & -q^2 - \alpha \end{bmatrix},$$

where

$$F(v) = \frac{v(1 + \sigma v)(1 - \kappa)}{(1 + v)(\kappa + v)^2}$$

and

$$H(v) = \frac{v}{\kappa + v}.$$

and that eigenvalues have negative real parts provided the following inequalities are satisfied:

$$\text{tr } \mathbf{J}_l - (1 + \rho)q^2 < 0,$$

$$\det \mathbf{J}_l + (\rho q^2 + \rho\alpha + \delta\bar{u}H(\bar{v}) - F(\bar{u}))q^2 > 0.$$

***(f)** Further discuss how diffusive *instability* might arise in this model. You may wish to refer to the analysis in Lauffenburger and Kennedy (1983).

8. Cells in the sluglike phase of *Dictyostelium discoideum* are either prespore or prestalk, and the two cell classes maintain a definite ratio despite experimental manipulations such as excision of part of the mass. Use a simple model outlined in Chapter 7 to suggest one type of mechanism that might lead to this ratio regulation. Comment on ways of testing such a model.

9. *Reaction-diffusion systems*

(a) Use Taylor-series expansions for R_1 and R_2 to show that equations (20a,b) lead to equations (24a,b) for *small* perturbations.

(b) Show that equations (24a,b) are equivalent to system (26a–d).

(c) Show that by assuming perturbations of the form (27) one arrives at equations (28a,b).

(d) Verify that equation (30) results.

(e) Use the inequality (33b) directly to reason that diffusion has the capacity to act as a destabilizing influence [*Hint:* note the effect of $D_i q^2$ on the self-influencing terms a_{ii}.]

10. **(a)** Show that the expression on the LHS of inequality (33b) corresponds to the quantity defined in equation (35).

(b) Demonstrate that $H(q^2)$ has a minimum, and prove that $q^2_{\min}$ is given by (36a) (*Hint:* Set $dH/dq^2 = 0$ and solve for $q^2_{\min}$.)

(c) Evaluate $H(q^2_{\min})$.

(d) Show that (34) implies (37).

(e) Derive inequality (38) from (37) and (32b).

(f) Verify that (38) can be written in the dimensionless form given in (39).

11. **(a)** Justify inequalities (40) and (41).

(b) Verify inequality (45). What are the dimensions of τ_1 and τ_2? of D_2/τ_2 and D_1/τ_1?

(c) Explain what is meant physically by the statement that the range of inhibition should be larger than the range of activation.

(d) Show that for (45) to hold it must also be true that $D_2 > D_1$.

(e) Explain the deduction that spacing between patterns will be approximately given by (46) at the onset of diffusive instability.

(f) Suggest what sort of biological influences might bring about the parameter variation that leads to diffusive instability.

***12.** The growth rate of a given wavenumber q_i is σ_i, and is given by (30). Describe how one could use this equation to solve for σ_i, and find the wavenumber of the *fastest*-growing perturbation.

13. Generalize the physical arguments given in Section 11.6 for the case of activator-inhibitor systems to the case of positive-feedback systems.

14. *Reaction-diffusion in two dimensions*

(a) Write out the linearized system corresponding to equations (48a,b).

(b) By explicitly differentiating equation (49) show that these are solutions to the linearized equations. Obtain a set of algebraic equations in α_1 and α_2 (involving σ, q_i, and other parameters.)

(c) An alternate assumption about perturbations is that they take the following form:

$$C_i'(x, t) = \alpha_i e^{\sigma t} \cos(q_1 x + q_2 y).$$

Use a trigonometric identity and boundary conditions (50a,b) to show that this is equivalent to equation (49).

(d) Verify that equation (53) is obtained for the quantity Q^2 characterizing the most destabilizing perturbations.

15. In the following problems you are given a set of reaction terms $R_1(c_1, c_2)$ and $R_2(c_1, c_2)$. Determine whether or not a homogeneous steady state can be obtained and whether the system is capable of giving rise to diffusive instability. If so, give explicit conditions for instability to arise, and determine which modes would be most destabilizing.

(a) Lotka-Volterra:
$R_1 = ac_1 - bc_1c_2,$
$R_2 = -ec_2 + dc_1c_2.$

(b) Species competition:
$R_1 = \mu_1 c_1 - \alpha_1 c_1^2 - \gamma_{12} c_1 c_2,$
$R_2 = \mu_2 c_2 - \alpha_2 c_2^2 - \gamma_{21} c_1 c_2,$
$\left(\frac{\mu_2}{\mu_1} < \frac{\gamma_{21}}{\alpha_1}, \quad \frac{\mu_2}{\mu_1} < \frac{\alpha_2}{\gamma_{12}}\right).$

(c) Glycolytic oscillator:
$R_1 = \delta - kc_1 - c_1c_2^2,$
$R_2 = kc_1 + c_1c_2^2 - c_2.$

(d) Schnakenberg chemical system:
$R_1 = c_1^2c_2 - c_1 + b,$
$R_2 = -c_1^2c_2 + a.$

(e) Van der Pol oscillator:
$R_1 = c_2 - \frac{c_1^3}{3} + c_1,$
$R_2 = -c_1.$

(f) Phytoplankton-herbivore system (Levin and Segel, 1976):
$R_1 = ac_1 + ec_1^2 - b_1c_1c_2,$
$R_2 = -dc_2^2 + b_2c_1c_2.$

(g) Tyson-Fife model for Belousov-Zhabotinsky reaction:
$R_1 = \frac{1}{\epsilon}\frac{c_1(1 - c_1) - bc_1(c_2 - a)}{c_2 + a},$
$R_2 = c_1 - c_2.$

(h) Meinhardt (1983) model:
$R_1 = ec_1^2c_2 - \mu c_1,$
$R_2 = e_0 - ec_1^2c_2.$

16. In this problem you are asked to explore the mechanism Meinhardt and Gierer suggested [equations (57a,b)] by using linear stability theory. Set $\rho_0 = \rho_1 = 0$ and assume that ρ' and ρ are constant.

(a) Suppose diffusion is absent. Draw a phase-plane portrait of the reaction scheme in equations (57a,b) and show the location of the nullclines and steady state $(\bar{A}, \bar{H})$.

(b) Using the conditions derived in this chapter, show that diffusive instability of a homogeneous steady state $(\bar{A}, \bar{H})$ is possible, and give the necessary conditions on the parameters.

17. **(a)** Interpret equations (58a,b) of the Gierer-Meinhardt model in terms of a hypothetical set of interacting chemicals a and h. Show that $c_1 = c_2 = c$ leads to dimensional inconsistency.

(b) Explain conditions (62a,b) in physical terms.

(c) Verify that (62b) implies (63). (*Hint:* Consider the equation $x - 1/x = 2$ and solve for x.)

18. Interpret the Segel-Jackson equations (66a,b) for a spatially distributed predator-prey system. Why would the term $-CE^2$ be described as a "combat" term?

(a) The authors claim that for $C = 0$ the model will not yield a diffusive instability. Justify and interpret this result.

(b) The assumption $M = 0$ does not prevent instability from occurring. Why?

(c) Assume that $M = 0$, in other words, that predator mortality from "combat" predominates over that due to other causes. Show that the equations can be written in the following dimensionless form:

$$\frac{\partial v}{\partial t} = (1 + kv)v - aev + \delta^2 \nabla^2 v,$$

$$\frac{\partial e}{\partial t} = ev - e^2 + \nabla^2 e,$$

where $e = EC/K_0$, $v = VB/K_0$, distances are scaled in units of $(\mu_2/K_0)^{-1/2}$ and time is scaled in units of K_0.

(d) Show that the dimensionless parameters appearing in part (c) are $k = K_1/B$, $a = A/C$, and $\delta^2 = \mu_1/\mu_2$. Interpret the meanings of these quantities.

(e) Show that the nontrivial steady state of this system is

$$e = v = \frac{1}{a - k}.$$

(f) Show that the instability condition is

$$k - \delta^2 > 2(a - k)^{1/2},$$

and that the wavenumber of the excitable modes is given by

$$Q^2 = \frac{1}{\delta(a - k)^{1/2}}.$$

19. *Effects of geometry on patterns formed.* Consider a rectangle of sides L_x and L_y where

$$L_x = L, \qquad L_y = \gamma L.$$

(a) Suppose that the boundaries are impermeable (that is, no flux boundary conditions apply). Show that the wavenumbers q_1 and q_2 of a perturbation in the x and y directions satisfy (51a,b).

(b) Suppose that the quantities L, D_{ij}, and a_{ij} are kept fixed but that the size proportion γ is gradually decreased. Interpret what effect this would have on the shape of the domain.

(c) Now assume that the *only* excitable modes are those satisfying (56). If initially $m = n = 4$ and $\gamma = 1$, determine the succession of modes (m_j, n_j) corresponding to a sequence of increasing values of γ.

(d) Draw several of these patterns.

20. *Effects of boundary conditions on patterns formed.* Now suppose that in problem 19 the boundaries are not impermeable but rather are artificially kept at the steady-state concentrations $\bar{C}_1$ and $\bar{C}_2$:

$$C_1(x, y, t) = \bar{C}_1 \qquad (x = 0, x = L, y = 0, y = \gamma L),$$

$$C_2(x, y, t) = \bar{C}_2 \qquad (x = 0, x = L, y = 0, y = \gamma L).$$

(a) How would this change the assumed form of the perturbations given by equation (49)?

(b) How would this affect the form of the wavenumbers given by (51a,b)?

(c) What effect would this have on expressions in (54) and (56)?

(d) Now consider mixed boundary conditions: constant concentrations along the x boundaries and no flux along the y boundaries. Repeat steps (a) through (c).

(e) In each of the above two cases, assume that $\gamma = 2$ and that the size of the region, L^2, is gradually increased (all else being held constant). Describe the succession of modes you might expect to encounter by drawing up a table analogous to the one in Figure 11.5.

21. *A model for animal coat patterns (Murray, 1981a)* In melanogenesis the precursor tyrosine is oxidized to dihydrophenylalanine (DOPA) in the presence of the enzyme tyrosinase. DOPA oxidizes further before the final polymerization to melanin. Murray (1981a) proposes that prepattern formation occurs before the arrival of *melanoblasts* (precursors of the melanin-producing *melanocytes*) at the epidermal surface. He considers two species, a high-molecular-weight substrate S and a cosubstrate A. For example, the substrate could be associated with tyrosine or the enzyme tyrosinase, and the cosubstrate might be an inhibitor governing melanogenesis initiation. The kinetics are taken to be that of substrate inhibition of an immobile enzyme. It is assumed that the two reactive species S and A are maintained at constant concentrations S_0 and A_0 in a reservoir. From this reservoir they diffuse through an inactive membrane of thickness L_1 onto an active membrane of thickness L_2. (See accompanying diagram.) The active membrane contains the immobile enzyme tyrosinase, which allows S and A to react at the following rate:

$$R = \frac{V_m AS}{K_m + S + S^2/K_S}, \tag{70}$$

where V_m, K_m, and K_S are assumed to be constant. Murray then suggests the following reaction-diffusion equations:

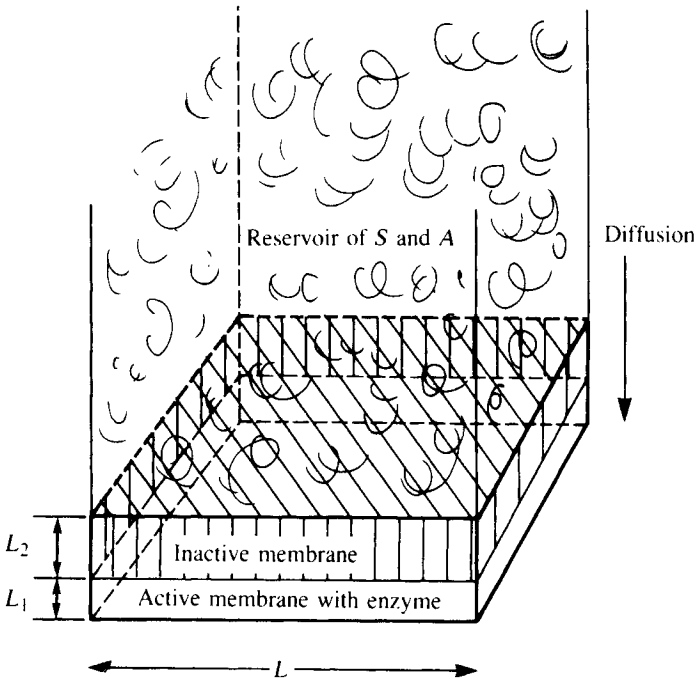

Figure for problem 21. S *and* A *diffuse from a reservoir to the active membrane, where they undergo an enzyme-catalyzed reaction. [Based on a drawing by Marjorie Buff.]*

$$\frac{\partial S}{\partial T} = \frac{D_S'}{L_1 L_2}(S_0 - S) - \frac{V_m A S}{K_m + S + S^2/K_S} + D_s \nabla^2 S, \qquad (71a)$$

$$\frac{\partial A}{\partial T} = \frac{D_A'}{L_1 L_2}(A_0 - A) - \frac{V_m A S}{K_m + S + S^2/K_S} + D_A \nabla^2 A, \qquad (71b)$$

where D_S' and D_A' are the diffusion coefficients for S and A in the inactive membrane, and D_S and D_A are the diffusion coefficients for S and A in the active layer.

(a) Explain reaction mechanism (70). (*Note:* You may find it useful to refer to problem 22 in Chapter 7.)

(b) Explain the various terms in equations (71a,b). [*Note:* Diffusive flux into the active membrane from the reservoir is proportional to $D_S'(S_0 - S)$ and $D_A'(A_0 - A)$.] Why does the product $L_1 L_2$ appear in this expression?

(c) Murray assumes that $D_S < D_A$. On what property of the substance S does he base this assumption? Why is such an assumption necessary?

(d) Define dimensionless variables as follows:

$$s = \frac{S}{K_m}, \qquad a = \frac{A}{K_m}, \qquad t^* = \frac{tD_S}{L_2}, \qquad \nabla^{*2} = L^2 \nabla^2.$$

Show that equations (71a,b) can be written in the dimensionless form given by equations (65a,b) of Section 11.8, where

$$f(s, a) = \alpha(a_0 - a) - \rho F(s, a), \qquad (72a)$$

$$g(s, a) = s_0 - s - \rho F(s, a), \tag{72b}$$

$$F(s, a) = \frac{sa}{1 + s + Ks^2}. \tag{72c}$$

(e) What are the dimensionless parameters α, β, γ, K, and ρ that appear in equations (65) and (72)? (For example, find that $K = K_m/K_s$, and so forth.)

(f) Interpret the biological significance of these parameters.

(g) Why is it not possible to obtain a simple analytical solution for the homogeneous steady state $(\bar{s}, \bar{a})$ of this model?

(h) Find the Jacobian matrix

$$\mathbf{J} = \begin{pmatrix} g_s & g_a \\ f_s & f_a \end{pmatrix}$$

for f and g given in part (d).

(i) Show that $\partial f/\partial a < 0$ and $\partial g/\partial a < 0$. What must be true about $\partial f/\partial s$ and $\partial g/\partial s$ at the steady state $(\bar{s}, \bar{a})$ if this chemical reaction is to exhibit diffusive instability? Which of the two types of chemical interactions given in Section 11.6 is consistent with the signs of the partial derivatives in **J**?

(j) Show that the requirements found in part (i) are consistent with $\bar{s} > 1\sqrt{K}$. Can you interpret this result biologically?

(k) It is not an easy task to graph the curves corresponding to the nullclines of this system. However, given that for three different K values the graphs have the qualitative features shown in Figures 8.6(*a*), it is a straightforward process to deduce which of these corresponds to a situation that implies diffusive instability. Use results of Section 7.8 to make this deduction.

22. *Diffusive predator-prey model (Mimura and Murray, 1978).* Consider the general model suggested by Mimura and Murray [equations (68a,b)]. Suppose $(\bar{P}, \bar{Q})$ stands for the homogeneous steady state of these equations.

(a) What are the equations of the nullclines in the spatially homogeneous equations? (What equations do $\bar{P}$ and $\bar{Q}$ satisfy?)

(b) Give conditions for stability of this steady state in the absence of diffusion. Determine the possible sign patterns of elements in the Jacobian.

(c) The two nullclines shown in Figure 11.17 intersect to the left of the hump in the P-nullcline. Is this configuration consistent with diffusive instability?

(d) Give the full condition for diffusive instability in this system.

REFERENCES

Reaction Diffusion and Models for Developmental Biology

Bard, J. B. L. (1977). A unity underlying the different zebra striping patterns. *J. Zool.* (London), *183*, 527–539.

Berding, C.; Harbich, T.; and Haken, H. (1983). A prepattern formation mechanism for the spiral-type patterns of the sunflower head. *J. Theor. Biol., 104,* 53–70.

Gierer, A., and Meinhardt, H. (1972). A theory of biological pattern formation. *Kybernetik, 12,* 30–39.

Kauffman, S. A. (1977). Chemical patterns, compartments, and a binary epigenetic code in *Drosophila. Am. Zool., 17,* 631–648.

Kauffman, S. A., Shymko, R. M., Trabert, K. (1978). Control of sequential compartment formation in Drosphila. *Science, 199,* 259.

Lacalli, T. C. (1981). Dissipative structures and morphogenetic pattern in unicellular algae. *Phil. Trans. Roy. Soc. Lond. B (Biol. Sci.), 294,* 547–588.

Lacalli, T. C., and Harrison, L. G. (1979). Turing's conditions and the analysis of morphogenetic models. *J. Theor. Biol., 76,* 419–436.

Meinhardt, H. (1978). Models for the ontogenetic development of higher organisms. *Rev. Physiol. Biochem. Pharmacol., 80,* 47–104.

Meinhardt, H. (1982). *Models of Biological Pattern Formation.* Academic Press, New York.

Meinhardt, H., and Gierer, A. (1974). Applications of a theory of biological pattern formation based on lateral inhibition. *J. Cell. Sci., 15,* 321–346.

Meinhardt, H., and Gierer, A. (1980). Generation and regeneration of sequence of structures during morphogenesis. *J. Theor. Biol., 85,* 429–450.

Murray, J. D. (1981*a*). A prepattern formation mechanism for animal coat markings. *J. Theor. Biol., 88,* 161–199.

Murray, J. D. (1981*b*). On pattern formation mechanisms for Lepidopteran wing patterns and mammalian coat markings. *Phil. Trans. R. Soc. Lond. B, 295,* 473–496.

Segel, L. A., ed. (1980). *Mathematical Models in Molecular and Cellular Biology.* Cambridge University Press, Cambridge.

Segel, L. A. (1984). *Modeling Dynamic Phenomena in Molecular and Cellular Biology.* Cambridge University Press, Cambridge, chap. 8.

Reaction Diffusion and Ecological Patterns

Conway, E. D. (1983). Diffusion and the predator-prey interaction: Pattern in closed systems. Tulane University Report in Computing and Applied Mathematics, New Orleans.

Mimura, M., and Murray, J. D. (1978). On a diffusive prey-predator model which exhibits patchiness. *J. Theor. Biol., 75,* 249–262.

Okubo, A. (1980). *Diffusion and Ecological Problems: Mathematical Models.* Springer-Verlag, New York.

Segel, L. A., and Jackson, J. L. (1972). Dissipative structure: An explanation and an ecological example. *J. Theor. Biol., 37,* 545–59.

Cellular Slime Molds and Mathematical Models

Bonner, J. T. (1944). A descriptive study of the development of the slime mold *Dictyostelium discoideum, Amer. J. Bot., 31,* 175–182.

Bonner, J. T. (1959). *The Cellular Slime Molds.* Princeton University Press, Princeton, N.J.

Bonner, J. T. (1974). *On Development; the biology of form.* Harvard University Press, Cambridge, Mass.

Devreotes, P. N., and Steck, T. L. (1979). Cyclic 3′5′ AMP relay in *Dictyostelium discoideum. J. Cell Biol., 80,* 300–309.

Goldbeter, A., and Segel, L. A. (1980). Control of developmental transitions in the cyclic AMP signalling system of *Dictyostelium discoideum. Differentiation, 17,* 127–135.

Keller, E. F., and Segel, L. A. (1970). The initiation of slime mold aggregation viewed as an instability. *J. Theor. Biol., 26,* 399–415.

Odell, G. M., and Bonner, J. T. (1986). How the Dictyostelium discoideum grex crawls. *Phil. Trans. Roy. Soc. Lond. B,* 312, 487–525.

Pate, E. F., and Odell, G. M. (1981). A computer simulation of chemical signaling during the aggregation phase of *Dictyostelium discoideum. J. Theor. Biol., 88,* 201–239.

Pate, E. F., and Othmer, H. G. (1986). Differentiation, cell sorting, and proportion regulation in the slug stage of *Dictyostelium discoideum. J. Theor. Biol., 118,* 301–319.

Rubinow, S. I., Segel, L. A.; Ebel, W. (1981). A mathematical framework for the study of morphogenetic development in the slime mold. *J. Theor. Biol., 91,* 99–113.

Segel, L. A. ed. (1980). *Mathematical Models in Molecular and Cellular Biology,* Cambridge University Press, Cambridge.

Segel, L. A. (1981). Analysis of population chemotaxis. Sect. 6.5 in Segel, L. A. ed. *Mathematical Models in Molecular and Cellular Biology,* Cambridge University Press, Cambridge, pp. 486–501.

Segel, L. A. (1984). *Modeling dynamic phenomena in molecular and cellular Biology,* (Chapter 6), Cambridge University Press, Cambridge.

Segel, L. A., and Stoeckly, B. (1972). Instability of a layer of chemotactic cells, attractant, and degrading enzyme. *J. Theor. Biol., 37,* 561–585.

Mathematical and General Sources

Fife, P. C. (1979). *Mathematical Aspects of Reacting and Diffusing Systems.* Springer-Verlag, New York.

Murray, J. D. (1982). Parameter space for Turing instability in reaction diffusion mechanisms: A comparison of models. *J. Theor. Biol., 98,* 143–163.

Rothe, F. (1984). *Global Solutions of Reaction-Diffusion Systems.* Springer-Verlag, Berlin.

Smoller, J. (1983). *Shock Waves and Reaction-Diffusion Equations.* Springer-Verlag, New York.

Tyson, J. J., and Fife, P. C. (1980). Target patterns in a realistic model of the Belousov-Zhabotinski reaction. *J. Chem. Phys., 73,* 2224–2237.

Reviews

Bard, J., and Lauder, I. (1974). How well does Turing's theory of morphogenesis work? *J. Theor. Biol., 45,* 501–531.

Levin, S., ed. (1983). *Modelling of Patterns in Space and Time.* Springer-Verlag, New York.

Levin, S. A., and Segel, L. A. (1985). Pattern generation in space and aspect. *SIAM Rev., 27,* 45–67.

Chemical Morphogens in Hydra

Kemmner, W. (1984). Head regeneration in *Hydra:* Biological studies and a model. In W. Jager and J. D. Murray, eds., *Modelling of Patterns in Space and Time.* Springer-Verlag, New York. (See also references therein.)

Other Pattern Formation Models

Ermentrout, G. B.; Campbell, J.; and Oster, G. (1986). A model for shell patterns based on neural activity. *Veliger, 28,* 369–388.

Ermentrout, G. B., and Cowan, J. D. (1979). A mathematical theory of visual hallucination patterns. *Biol. Cybernet., 34,* 137–150.

Ermentrout, G. B. (1984). Mathematical models for the patterns of premigrainous auras, in A. V. Holden and W. Winlow, eds., *The Neurobiology of Pain,* Manchester University Press, Manchester, England.

Cohen, D. (1967). Computer simulation of biological pattern generation processes. *Nature, 216,* 246–248.

Jackson, J. B. C.; Buss, L. W.; and Cook, R. E., ed. (1985). *Population Biology and Evolution of Clonal Organisms.* Yale University Press, New Haven, Conn.

Murray, J. D., and Oster, G. F. (1984). Cell traction models for generating pattern and form in morphogenesis. *J. Math. Biol., 19,* 265–279.

Nijhout, H. F. (1981). The color patterns of butterflies and moths. *Sci. Am.,* November 1981, pp. 140–151.

Odell, G. M.; Oster, G.; Alberch, P.; and Burnside, B. (1981). The mechanical basis of morphogenesis. *Develop. Biol., 85,* 446–462.

Oster, G. F.; Murray, J. D.; and Harris, A. K. (1983). Mechanical aspects of mesenchymal morphogenesis. *J. Embryol. Exp. Morph., 78,* 83–125.

Sulsky, D.; Childress, S.; and Percus, J. K. (1984). A model of cell sorting. *J. Theor. Biol., 106,* 275–301.

Swindale, N. V. (1980). A model for the formation of ocular dominance stripes. *Proc. R. Soc. Lond. B, 208,* 243–264.

Thompson, D'Arcy, W. (1942). *On Growth and Form.* Cambridge University Press, Cambridge.

Young, D. A. (1984). A local activator-inhibitor model of vertebrate skin patterns. *Math. Biosci., 72,* 51–58.

Wolfram, S. (1984*a*). Cellular automata as models of complexity. *Nature, 311,* 419–424.

Wolfram, S. (1984*b*). Universality and complexity in cellular automata. *Physica, 10D,* 1–35.

Miscellaneous

Lauffenburger, D. A., and Kennedy, C. R. (1983). Localized bacterial infection in a distributed model for tissue inflammation. *J. Math. Biol., 16,* 141–163.

Schaller, H. C. (1973). Isolation and characterization of a low molecular weight substance activating head and bud formation in hydra. *J. Embryol. Exp. Morphol., 29,* 27–38.

Schaller, H. C. (1976). Action of the head activator on the determination of interstitial cells in hydra. *Cell. Differ. 5,* 13–20.

Nicolis, G., and Prigogine, I. (1977). *Self-Organization in Nonequilibrium Systems.* Wiley, New York.